Séminaire Poincaré 2 (2002) 93 – 125

Séminaire Poincaré

The Anomalous Magnetic Moments of the Electron and the Muon

Marc Knecht
Centre de Physique Théorique
CNRS-Luminy, Case 907
F-13288 Marseille Cedex 9, France

1 Introduction

In February 2001, the Muon (g-2) Collaboration of the E821 experiment at the Brookhaven AGS released a new value of the anomalous magnetic moment of the muon, measured with an unprecedented accuracy of 1.3 ppm. This announcement has caused quite some excitement in the particle physics community. Indeed, this experimental value was claimed to show a deviation of 2.6 σ with one of the most accurate evaluation of the anomalous magnetic moment of the muon within the standard model. It was subsequently shown that a sign error in one of the theoretical contributions was responsible for a sizable part of this discrepancy, which eventually only amounted to 1.6 σ. However, this event had the merit to draw the attention to the fact that low energy but high precision experiments represent real potentialities, complementary to the high energy accelerator programs, for evidencing possible new degrees of freedom, supersymmetry or whatever else, beyond those described by the standard model of electromagnetic, weak, and strong interactions.

Clearly, in order for theory to match such an accurate measurement [in the meantime, the relative error has even been further reduced, to 0.7 ppm], calculations in the standard model have to be pushed to their very limits. The difficulty is not only one of having to compute higher orders in perturbation theory, but also to correctly take into account strong interaction contributions involving low-energy scales, where non perturbative effects are important, and which therefore represent a real theoretical challenge.

The purpose of this account is to give an overview of the main features of the theoretical calculations that have been done in order to obtain accurate predictions for the anomalous magnetic moments of the electron and of the muon within the standard model. There exist several excellent reviews of the subject, which the interested reader may consult. As far as the situation up to 1990 is concerned, the collection of articles published in Ref. [1] offers a wealth of information, on both theory and experiment. A very useful account of earlier theoretical work is presented in Ref. [2]. Among the more recent reviews, Refs. [3, 4, 5, 6] are most informative. I shall not touch on the subject of the study of new physics scenarios which might offer an explanation for a possible deviation between the standard model prediction of the magnetic moment of the muon and its experimental value. For this aspect, I refer the reader to [7] and to the articles quoted therein, or to [8].

2 General considerations

In the context of relativistic quantum mechanics, the interaction of a pointlike spin one-half particle of charge e_ℓ and mass m_ℓ with an external electromagnetic field $\mathcal{A}_\mu(x)$ is described by the Dirac equation with the minimal coupling prescription,

$$i\hbar\,\frac{\partial\psi}{\partial t} \;=\; \left[c\boldsymbol{\alpha}\cdot\left(-i\hbar\boldsymbol{\nabla}-\frac{e_\ell}{c}\boldsymbol{\mathcal{A}}\right)+\beta m_\ell c^2+e_\ell\mathcal{A}_0\right]\psi\,. \tag{2.1}$$

In the non relativistic limit, this reduces to the Pauli equation for the two-component spinor φ describing the large components of the Dirac spinor ψ,

$$i\hbar\,\frac{\partial\varphi}{\partial t}\;=\;\left[\frac{(-i\hbar\boldsymbol{\nabla}-(e_\ell/c)\boldsymbol{\mathcal{A}})^2}{2m_\ell}\;-\;\frac{e_\ell\hbar}{2m_\ell c}\,\boldsymbol{\sigma}\cdot\mathrm{B}\;+\;e_\ell\mathcal{A}_0\right]\varphi\,. \tag{2.2}$$

As is well known, this equation amounts to associate with the particle's spin a magnetic moment

$$\mathrm{M}_s\;=\;g_\ell\,\left(\frac{e_\ell}{2m_\ell c}\right)\,\mathrm{S}\,,\;\mathrm{S}=\hbar\,\frac{\boldsymbol{\sigma}}{2}\,, \tag{2.3}$$

with a gyromagnetic ratio predicted to be $g_\ell = 2$.

In the context of quantum field theory, the response to an external electromagnetic field is described by the matrix element of the electromagnetic current [1]$\mathcal{J}^\rho$ [spin projections and Dirac indices are not written explicitly]

$$\langle\ell^-(p')|\mathcal{J}^\rho(0)|\ell^-(p)\rangle\;=\;\bar{\mathrm{u}}(p')\Gamma^\rho(p',p)\mathrm{u}(p)\,, \tag{2.4}$$

with $[k_\mu\equiv p'_\mu-p_\mu]$

$$\Gamma^\rho(p',p)\;=\;F_1(k^2)\gamma^\rho\;+\;\frac{i}{2m_\ell}\,F_2(k^2)\sigma^{\rho\nu}k_\nu\;-\;F_3(k^2)\gamma_5\sigma^{\rho\nu}k_\nu\,. \tag{2.5}$$

This expression of the matrix element $\langle\ell^-(p')|\mathcal{J}^\rho(0)|\ell^-(p)\rangle$ is the most general that follows from Lorentz invariance, the Dirac equation for the two spinors, $(\not{p}-m)\mathrm{u}(p)=0$, $\bar{\mathrm{u}}(p')(\not{p}'-m)=0$, and the conservation of the electromagnetic current, $(\partial\cdot\mathcal{J})\,(x)\,=0$. The two first form factors, $F_1(k^2)$ and $F_2(k^2)$, are known as the Dirac (or electric) form factor and the Pauli (or magnetic) form factor, respectively. Since the electric charge operator $\mathcal{Q}$ is given, in units of the charge e_ℓ, by

$$\mathcal{Q}\;=\;\int d\mathrm{x}\,\mathcal{J}_0(x^0,\mathrm{x})\,, \tag{2.6}$$

the form factor $F_1(k^2)$ satisfies the normalization condition $F_1(0)=1$. The presence of the form factor $F_3(k^2)$ requires both parity and time reversal invariance to be broken. It is therefore absent if only electromagnetic interactions are considered. On the other hand, in the standard model, the weak interactions violate both parity and time reversal symmetry, so that they may induce such a form factor.

The analytic structure of these form factors is dictated by general properties of quantum field theory [causality, analyticity, and crossing symmetry]. They are real functions of k^2 in the spacelike region $k^2<0$. In the timelike region, they become complex, with a cut starting at $k^2>4m_\ell^2$. At $k^2=0$, they describe the residue of the s-channel pole in the S-matrix element for elastic $\ell^+\ell^-$ scattering.

At tree level, i.e. in the classical limit, one finds

$$F_1^{\mathrm{tree}}(k^2)=1\,,\;F_2^{\mathrm{tree}}(k^2)=0\,,\;F_3^{\mathrm{tree}}(k^2)=0\,. \tag{2.7}$$

In order to obtain non zero values for $F_2(k^2)$ and $F_3(k^2)$ already at tree level, the interaction of the Dirac field with the photon field $\mathcal{A}_\mu$ would have to depart from the minimal coupling prescription. For instance, the modification $[\mathcal{F}_{\mu\nu}=\partial_\mu\mathcal{A}_\nu-\partial_\nu\mathcal{A}_\mu,\,\mathcal{J}^\rho=\overline{\psi}\gamma^\rho\psi]$

$$\begin{aligned}\int d^4x\mathcal{L}_{\mathrm{int}}\;&=\;-\frac{e_\ell}{c}\int d^4x\mathcal{J}^\rho\mathcal{A}_\rho\;\rightarrow\\ \rightarrow\;\int d^4x\widehat{\mathcal{L}}_{\mathrm{int}}\;&=\;-\frac{e_\ell}{c}\int\left[\mathcal{J}^\rho\mathcal{A}_\rho+\frac{\hbar}{4m_\ell}a_\ell\overline{\psi}\sigma_{\mu\nu}\psi\mathcal{F}^{\mu\nu}+\frac{\hbar}{2e_\ell}d_\ell\overline{\psi}i\gamma_5\sigma_{\mu\nu}\psi\mathcal{F}^{\mu\nu}\right]\\ &=\;-\frac{e_\ell}{c}\int d^4x\widehat{\mathcal{J}}^\rho\mathcal{A}_\rho\,,\end{aligned} \tag{2.8}$$

[1] In the standard model, $\mathcal{J}^\rho$ denotes the total electromagnetic current, with the contributions of all the charged elementary fields in presence, leptons, quarks, electroweak gauge bosons,...

with [2]

$$\widehat{\mathcal{J}}_\rho \;=\; \mathcal{J}_\rho - \frac{\hbar}{2m_\ell} a_\ell \partial^\mu \left(\overline{\psi}\sigma_{\mu\rho}\psi\right) - \frac{\hbar}{d_\ell} e_\ell \partial^\mu \left(\overline{\psi} i\gamma_5 \sigma_{\mu\rho}\psi\right) , \tag{2.9}$$

leads to

$$\widehat{F}_1^{\,\mathrm{tree}}(k^2) = 1\,,\;\; \widehat{F}_2^{\,\mathrm{tree}}(k^2) = a_\ell\,,\;\; \widehat{F}_3^{\,\mathrm{tree}}(k^2) = d_\ell/e_\ell\,. \tag{2.10}$$

The equation satisfied by the Dirac spinor ψ then reads

$$\begin{aligned} i\hbar\,\frac{\partial\psi}{\partial t} \;=\; \Big[& c\boldsymbol{\alpha}\cdot\left(-i\hbar\boldsymbol{\nabla} - \frac{e_\ell}{c}\boldsymbol{\mathcal{A}}\right) + \beta m_\ell c^2 + e_\ell \mathcal{A}_0 \\ & + \frac{e_\ell\hbar}{2m_\ell}\, a_\ell \beta \left(i\boldsymbol{\alpha}\cdot \mathrm{E} - \boldsymbol{\Sigma}\cdot \mathrm{B}\right) - \hbar d_\ell \beta \left(\boldsymbol{\Sigma}\cdot \mathrm{E} + i\boldsymbol{\alpha}\cdot \mathrm{B}\right)\Big]\psi\,, \end{aligned} \tag{2.11}$$

and the corresponding non relativistic limit becomes [3]

$$i\hbar\,\frac{\partial\varphi}{\partial t} \;=\; \left[\frac{(-i\hbar\boldsymbol{\nabla} - (e_\ell/c)\boldsymbol{\mathcal{A}})^2}{2m_\ell} \;-\; \frac{e_\ell\hbar}{2m_\ell c}\,(1+a_\ell)\boldsymbol{\sigma}\cdot \mathrm{B}\cdot \mathrm{E} \;+\; e_\ell \mathcal{A}_0 \;+\; \cdots\right]\varphi\,. \tag{2.12}$$

Thus the coupling constant a_ℓ induces a shift in the gyromagnetic factor, $g_\ell = 2(1+a_\ell)$, while d_ℓ gives rise to an electric dipole moment. The modification (2.8) of the interaction with the photon field introduces two arbitrary constants, and both terms produces a *non renormalizable* interaction. Non constant values of the form factors could be generated at tree level upon introducing [9] additional non renormalizable couplings, involving derivatives of the external field of the type $\Box^n \mathcal{A}_\mu$, which preserve the gauge invariance of the corresponding field equation satisfied by ψ. In a renormalizable framework, like QED or the standard model, calculable non vanishing values for $F_2(k^2)$ and $F_3(k^2)$ are generated by the loop corrections. In particular, the latter will likewise induce an *anomalous magnetic moment*

$$a_\ell = \frac{1}{2}(g_\ell - 2) = F_2(0) \tag{2.13}$$

and an electric dipole moment $d_\ell = e_\ell F_3(0)$.

If we consider only the electromagnetic and the strong interactions, the current $\mathcal{J}^\rho$ is gauge invariant, and the two form factors symmetry $F_1(k^2)$ and $F_2(k^2)$ do not depend on the gauges chosen in order to quantize the photon and the gluon gauge fields. This is no longer the case if the weak interactions are included as well, since $\mathcal{J}^\rho$ now transforms under a weak gauge transformation, and the corresponding form factors in general depend on the gauge choices. As we have already mentioned above, the zero momentum transfer values $F_i(0)$, $i = 1,2,3$ describe a physical S-matrix element. To the extent that the perturbative S-matrix of the standard model does not depend on the gauge fixing parameters to any order of the renormalized perturbation expansion, the quantities $F_i(0)$ should define *bona fide* gauge-fixing independent observables.

The computation of $\Gamma_\rho(p',p)$ is often a tedious task, especially if higher loop contributions are considered. It is therefore useful to concentrate the efforts on computing the form factor of interest, e.g. $F_2(k^2)$ in the case of the anomalous magnetic moment. This can be achieved upon projecting out the different form factors [10, 11] using the following general expression [4]

$$F_i(k^2) \;=\; \mathrm{tr}\left[\Lambda_i^\rho(p',p)(\not{p}' + m_\ell)\Gamma_\rho(p',p)(\not{p} + m_\ell)\right]\,, \tag{2.14}$$

with

$$\Lambda_1^\rho(p',p) \;\;=\;\; \frac{1}{4}\,\frac{1}{k^2 - 4m_\ell^2}\,\gamma^\rho \;+\; \frac{3m_\ell}{2}\,\frac{1}{(k^2-4m_\ell^2)^2}\,(p'+p)^\rho$$

[2] The current $\widehat{\mathcal{J}}^\rho$ is still a conserved four-vector, therefore the matrix element $\langle \ell^-(p')|\widehat{\mathcal{J}}^\rho(0)|\ell^-(p)\rangle$ also takes the form (2.4), (2.5), with appropriate form factors $\widehat{F}_i(k^2)$.

[3] Terms involving the gradients of the external fields $\mathbf{E}$ and $\mathbf{B}$ or terms nonlinear in these fields are not shown.

[4] From now on, I most of the time use the system of units where $\hbar = 1$, $c = 1$.

$$\begin{aligned}\Lambda_2^\rho(p',p) &= -\frac{m_\ell^2}{k^2}\,\frac{1}{k^2-4m_\ell^2}\,\gamma^\rho - \frac{m_\ell}{k^2}\,\frac{k^2+2m_\ell^2}{(k^2-4m_\ell^2)^2}\,(p'+p)^{\,rho}\\ \Lambda_3^\rho(p',p) &= -\frac{i}{2k^2}\,\frac{1}{k^2-4m_\ell^2}\,\gamma_5(p'+p)^\rho\,. \end{aligned} \tag{2.15}$$

For $k \to 0$, one has

$$\Lambda_2^\rho(p,p') = \frac{1}{4k^2}\left[\gamma^\rho - \frac{1}{m_\ell}\left(1+\frac{k^2}{m_\ell^2}\right)(p+\frac{1}{2}k)^\rho + \cdots\right], \tag{2.16}$$

and

$$(\not p + m_\ell)\Lambda_2^\rho(p,p')(\not p' + m_\ell) = \frac{1}{4}(\not p + m_\ell)\left[-\frac{k^\rho}{k^2} + (\gamma^\rho - \frac{p^\rho}{m_\ell})\frac{\not k}{k^2} + \cdots\right]. \tag{2.17}$$

The last expression behaves as $\sim 1/k$ as the external photon four momentum k_μ vanishes, so that one may worry about the finiteness of $F_2(0)$ obtained upon using Eq. (2.14). This problem is solved by the fact that $\Gamma^\rho(p',p)$ satisfies the Ward identity

$$(p'-p)_\rho\Gamma^\rho(p',p) = 0\,, \tag{2.18}$$

following from the conservation of the electromagnetic current. Therefore, the identity

$$\Gamma^\rho(p',p) = -k_\sigma\,\frac{\partial}{\partial k_\rho}\,\Gamma^\sigma(p',p) \tag{2.19}$$

provides the additional power of k which ensures a finite result as $k_\mu \to 0$.

The presence of three different interactions in the standard model naturally leads one to consider the following decomposition of the anomalous magnetic moment a_ℓ:

$$a_\ell = a_\ell^{\rm QED} + a_\ell^{\rm had} + a_\ell^{\rm weak}\,. \tag{2.20}$$

By $a_\ell^{\rm QED}$, I denote all the contributions which arise from loops involving only virtual photons and leptons. Among these, it is useful to distinguish those which involve only the same lepton flavour ℓ for which we wish to compute the anomalous magnetic moment, and those which involve loops with leptons of different flavours, denoted collectively as ℓ' [$\alpha \equiv e^2/4\pi$],

$$a_\ell^{\rm QED} = \sum_{n\geq 1} A_n\left(\frac{\alpha}{\pi}\right)^n + \sum_{n\geq 2} B_n(\ell,\ell')\left(\frac{\alpha}{\pi}\right)^n. \tag{2.21}$$

The second type of contribution, $a_\ell^{\rm had}$ involves also quark loops. Their contribution is far from being limited to the short distance scales, and $a_\ell^{\rm had}$ is an intrinsically non perturbative quantity. From a theoretical point of view, this represents a serious difficulty. Finally, at some level of precision, the weak interactions can no longer be ignored, and contributions of virtual Higgs or massive gauge boson degrees of freedom induce the third component $a_\ell^{\rm weak}$. Of course, starting from the two loop level, a hadronic contribution to $a_\ell^{\rm weak}$ will also be present. The remaining of this presentation is devoted to a detailed discussion of these various contributions.

Before starting this guided tour of the anomalous magnetic moments of the massive charged leptons of the standard model, it is useful to keep in mind a few simple and elementary considerations:

• The anomalous magnetic moment is a dimensionless quantity. Therefore, the coefficients A_n above are *universal*, i.e. they do not depend on the flavour of the lepton whose anomalous magnetic moment we wish to evaluate.

• The contributions to a_ℓ of degrees of freedom corresponding to a typical scale $M \gg m_\ell$ decouple [12], i.e. they are *suppressed* by powers of m_ℓ/M.[5]

• The contributions to a_ℓ originating from light degrees of freedom, characterized by a typical scale $m \ll m_\ell$ are *enhanced* by powers of $\ln(m_\ell/m)$. At a given order, the logarithmic terms that do not vanish as $m_\ell/m \to 0$ can often be computed from the knowledge of the lesser order terms and of the β function through the renormalization group equations [15, 16, 17, 18].

These general properties already allow to draw a few elementary conclusions. The electron being the lightest charged lepton, its anomalous magnetic moment is dominantly determined by the values of the coefficients A_n. The first contribution of other degrees of freedom comes from graphs involving, say, at least one muon loop, which occurs first at the two-loop level, and is of the order of $(m_e^2/m_\mu)^2(\alpha/\pi)^2 \sim 10^{-10}$. The hadronic effects, i.e. "quark and gluon loops", characterized by a scale of ~ 1 GeV, or effects of degrees of freedom beyond the standard model, which may appear at some high scale M, will be felt more strongly, by a considerable factor $(m_\mu/m_e)^2 \sim 40\,000$, in a_μ than in a_e. Thus, a_e is well suited for testing the validity of QED at higher orders, whereas a_μ is more appropriate for detecting new physics. If we follow this line reasoning, a_τ would even be better suited for finding evidence of degrees of freedom beyond the standard model. Unfortunately, the very short lifetime of the τ lepton [$\tau_\tau \sim 3 \times 10^{-13} s$] makes a sufficiently accurate measurement of a_τ impossible at present.

3 Brief overview of the experimental situation

3.1 Measurements of the magnetic moment of the electron

The first indication that the gyromagnetic factor of the electron is different from the value $g_e = 2$ predicted by the Dirac theory came from the precision measurement of hyperfine splitting in hydrogen and deuterium [19]. The first measurement of the gyromagnetic factor of free electrons was performed in 1958 [20], with a precision of 3.6%. The situation began to improve with the introduction of experimental setups based on the Penning trap. Some of the successive values obtained over a period of forty years are shown in Table 1. Technical improvements, eventually allowing for the trapping of a single electron or positron, produced, in the course of time, an enormous increase in precision which, starting from a few percents, went through the ppm [parts per million] levels, before culminating at 4 ppb [parts per billion] [21] in the last of a series of experiments performed at the University of Washington in Seattle. The same experiment has also produced a measurement of the magnetic moment of the positron with the same accuracy, thus providing a test of CPT invariance at the level of 10^{-12},

$$g_{e^-}/g_{e^+} \;=\; 1 \;+\; (0.5 \pm 2.1) \times 10^{-12}\,. \tag{3.1}$$

An extensive survey of the literature and a detailed description of the various experimental aspects can be found in [22]. The earlier experiments are reviewed in [23].

3.2 Measurements of the magnetic moment of the muon

The anomalous magnetic moment of the muon has also been the subject of quite a few experiments. The very short lifetime of the muon, $\tau_\mu = (2.19703 \pm 0.00004) \times 10^{-6} s$, makes it necessary to proceed in a completely different way in order to attain a high precision. The experiments conducted at CERN during the years 1968-1977 used a muon storage ring [for details, see [31] and references quoted therein]. The more recent experiments at the AGS in Brookhaven are based on the same

[5] In the presence of the weak interactions, this statement has to be reconsidered, since the necessity for the cancellation of the $SU(2) \times U(1)$ gauge anomalies transforms the decoupling of, say, a single heavy fermion in a given generation, into a somewhat subtle issue [13, 14].

Table 1: Some experimental determinations of the electron's anomalous magnetic moment a_e with the corresponding relative precision.

0.001 19(5)	4.2%	[24]
0.001 165(11)	1%	[25]
0.001 116(40)	3.6%	[20]
0.001 160 9(2 4)	2 100 ppm	[26]
0.001 159 622(27)	23 ppm	[27]
0.001 159 660(300)	258 ppm	[28]
0.001 159 657 7(3 5)	3 ppm	[29]
0.001 159 652 41(20)	172 ppb	[30]
0.001 159 652 188 4(4 3)	4 ppb	[21]

concept. Pions are produced by sending a proton beam on a target. The pions subsequently decay into longitudinally polarized muons, which are captured inside a storage ring, where they follow a circular orbit in the presence of both a uniform magnetic field and a quadrupole electric field, the latter serving the purpose of focusing the muon beam. The difference between the spin precession frequency and the orbit, or synchrotron, frequency is given by

$$\boldsymbol{\omega}_s - \boldsymbol{\omega}_c = \frac{e}{m_\mu c}\left\{a_\mu \mathrm{B} - \left[a_\mu - \frac{1}{1-\gamma^2}\right]\boldsymbol{\beta}\wedge\mathrm{E}\right\}. \tag{3.2}$$

Therefore, if the Lorentz factor γ is tuned to its "magic" value $\gamma = \sqrt{1+1/a_\mu} = 29.3$, the measurement of $\omega_s - \omega_c$ and of the magnetic field B allows to determine a_μ. The spin direction of the muon is determined by detecting the electrons or positrons produced in the decay of the muons with an energy greater than some threshold energy E_t. The number of electrons detected decreases exponentially in time, with a time constant set by the muon's lifetime, and is modulated by the frequency $\omega_s - \omega_c$,

$$N_e(t) = N_0 e^{-t/\tau_\mu}\{1 + A\cos[(\omega_s - \omega_c)t + \phi]\}. \tag{3.3}$$

Table 2: Determinations of the anomalous magnetic moment of the positively charged muon from the storage ring experiments conducted at the CERN PS and at the BNL AGS.

0.001 166 16(31)	265 ppm	[32]
0.001 165 895(27)	23 ppm	[33]
0.001 165 911(11)	10 ppm	[34]
0.001 165 925(15)	13 ppm	[35]
0.001 165 9191(59)	5 ppm	[36]
0.001 165 920 2(16)	1.3 ppm	[37]
0.001 165 920 3(8)	0.7 ppm	[38]

Several experimental results for the anomalous magnetic moment of the positively charged muon, obtained at the CERN PS or, more recently, at the BNL AGS, are recorded in Table 2. Notice that the relative errors are measured in ppm units, to be contrasted with the ppb level of accuracy achieved in the electron case. The four last values in Table 2 were obtained by the E821 experiment at BNL. They show a remarkable stability and a steady increase in precision, and now completely

dominate the world average value. Further data, for negatively charged muons [6] are presently being analyzed. The aim of the Brookhaven Muon (g - 2) Collaboration is to reach a precision of 0.35 ppm, but this will depend on whether the experiment will receive financial support to collect more data or not.

3.3 Experimental bounds on the anomalous magnetic moment of the τ lepton

As already mentioned, the very short lifetime of the τ precludes a measurement of its anomalous magnetic moment following any of the techniques described above. Indirect access to a_τ is provided by the reaction $e^+e^- \to \tau^+\tau^-\gamma$. The results obtained by OPAL [39] and L3 [40] at LEP only provide very loose bounds,

$$\begin{aligned} -0.052 < a_\tau < 0.058 \ (95\% C.L.) \\ -0.068 < a_\tau < 0.065 \ (95\% C.L.)\,, \end{aligned} \tag{3.4}$$

respectively.

We shall now turn towards theory, in order to see how the standard model predictions compare with these experimental values. Only the cases of the electron and of the muon will be treated in some detail. The theoretical aspects as far as the anomalous magnetic moment of the τ are concerned are discussed in [41].

4 The anomalous magnetic moment of the electron

We start with the anomalous magnetic moment of the lightest charged lepton, the electron. Since the electron mass m_e is much smaller than any other mass scale present in the standard model, the mass independent part of $a_e^{\rm QED}$ dominates its value. As mentioned before, non vanishing contributions appear at the level of the loop diagrams shown in Fig. 1.

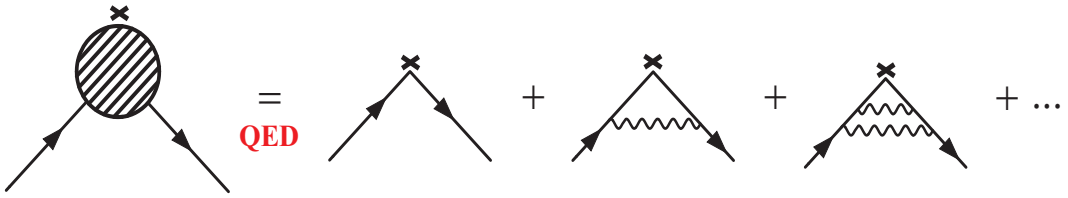

Figure 1: The perturbative expansion of $\Gamma^\rho(p',p)$ in single flavour QED. The tree graph gives $F_1 = 1$, $F_2 = F_3 = 0$. The one loop vertex correction graph gives the coefficient A_1 in Eq. (2.21). The cross denotes the insertion of the external field.

4.1 The lowest order contribution

The one loop diagram gives

$$\begin{aligned} \Gamma^\rho(p',p)\big|_{1\ \rm loop} &= (-ie)^2 \int \frac{d^4q}{(2\pi)^4} \gamma_\mu (\not{p}' + \not{q} + m_e) \gamma^\rho (\not{p} + \not{q} + m_e) \gamma^\mu \\ &\quad \times \frac{i}{(p'+q)^2 - m_e^2} \frac{i}{(p+q)^2 - m_e^2} \frac{(-i)}{q^2}\,. \end{aligned} \tag{4.1}$$

[6] The CERN experiment had also measured $a_{\mu^-} = 0.001\,165\,937(12)$ with a 10 ppm accuracy, giving the average value $a_\mu = 0.001\,165\,924(8.5)$, with an accuracy of 7 ppm.

The form factor $F_2(k^2)$ is obtained by using Eqs. (2.14) and (2.15) and, upon evaluating the corresponding trace of Dirac matrices, one finds

$$\begin{aligned} F_2(k^2)\big|_{1\text{ loop}} &= ie^2\,\frac{32m_e^2}{k^2(k^2-4m_e^2)^2}\int\frac{d^4q}{(2\pi)^4}\,\frac{1}{(p'+q)^2-m_e^2}\,\frac{1}{(p+q)^2-m_e^2}\,\frac{1}{q^2} \\ &\quad\times\left[-3k^2(p\cdot q)^2+2k^2m_e^2(p\cdot q)+k^2m_e^2q^2-m_e^2(k\cdot q)^2\right]. \end{aligned} \tag{4.2}$$

Then follow the usual steps of introducing two Feynman parameters, of performing a trivial change of variables and a symmetric integration over the loop momentum q, so that one arrives at

$$\begin{aligned} F_2(k^2)\big|_{1\text{ loop}} &= ie^2\,\frac{64m_e^2}{(k^2-4m_e^2)^2}\int_0^1 dx\,x\int_0^1 dy\int\frac{d^4q}{(2\pi)^4}\,\frac{1}{(q^2-\mathcal{R}^2)^3} \\ &\quad\times\left[2x(1-x)m_e^4-\frac{3}{4}x^2y^2(k^2)^2+m_e^2k^2x\left(3xy-y+\frac{1}{2}x\right)\right] \\ &= \frac{e^2}{\pi^2}\,\frac{2m_e^2}{(k^2-4m_e^2)^2}\int_0^1 dx\,x\int_0^1 dy\,\frac{1}{\mathcal{R}^2} \\ &\quad\times\left[2x(1-x)m_e^4-\frac{3}{4}x^2y^2(k^2)^2+m_e^2k^2x\left(3xy-y+\frac{1}{2}x\right)\right], \end{aligned} \tag{4.3}$$

with

$$\mathcal{R}^2 = x^2y(1-y)(2m_e^2-k^2)+x^2y^2m_e^2+x^2(1-y)^2m_e^2\,. \tag{4.4}$$

As expected, the limit $k^2\to 0$ can be taken without problem, and gives

$$a_e\big|_{1\text{ loop}} \equiv F_2(0)\big|_{1\text{ loop}} = \frac{1}{2}\,\frac{\alpha}{\pi}\,. \tag{4.5}$$

Let us stress that although the integral (4.1) diverges, we have obtained a finite result for $F_2(k^2)$, and hence for a_e, without introducing any regularization. This is of course expected, since a divergence in, say, $F_2(0)$ would require that a counterterm of the form given by the second term in $\widehat{\mathcal{L}}_{\text{int}}$, see Eq. (2.8), be introduced. This would in turn spoil the renormalizability of the theory. In fact, as is well known, the divergence lies in $F_1(0)$, and is absorbed into the renormalization of the electron's charge.

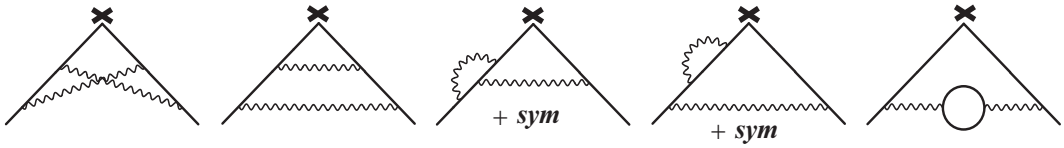

Figure 2: The Feynman diagrams which contribute to the coefficient A_2 in Eq. (2.21).

4.2 Higher order mass independent corrections

The previous calculation is rather straightforward and amounts to the result

$$A_1 = \frac{1}{2} \tag{4.6}$$

first obtained by Schwinger [42]. Schwinger's calculation was soon followed by a computation of A_2 [43], which requires the evaluation of 7 graphs, representing five distinct topologies, and shown in Fig. 2. Historically, the result of Ref. [43] was important, because it provided the first explicit example of the realization of the renormalization program of QED at two loops. However, the

value for A_2 was not given correctly. The correct expression of the second order mass independent contribution was derived in [44, 45, 46] (see also [47, 48]) and reads [7]

$$\begin{aligned} A_2 &= \frac{197}{144} + \left(\frac{1}{2} - 3\ln 2\right)\zeta(2) + \frac{3}{4}\zeta(3) \\ &= -0.328\,478\,965... \end{aligned} \tag{4.7}$$

with $\zeta(p) = \sum_{n=1}^{\infty} 1/n^p$, $\zeta(2) = \pi^2/6$. The occurrence of transcendental numbers like zeta functions or polylogarithms is a general feature of higher order calculations in perturbative quantum field theory. The pattern of these transcendentals in perturbation theory has also been put in relationship with other mathematical structures, like knot theory.

The analytic evaluation of the three-loop mass independent contribution to the anomalous magnetic moment required quite some time, and is mainly due to the dedication of E. Remiddi and his coworkers during the period 1969-1996. There are now 72 diagrams to consider, involving many different topologies, see Fig. 3.

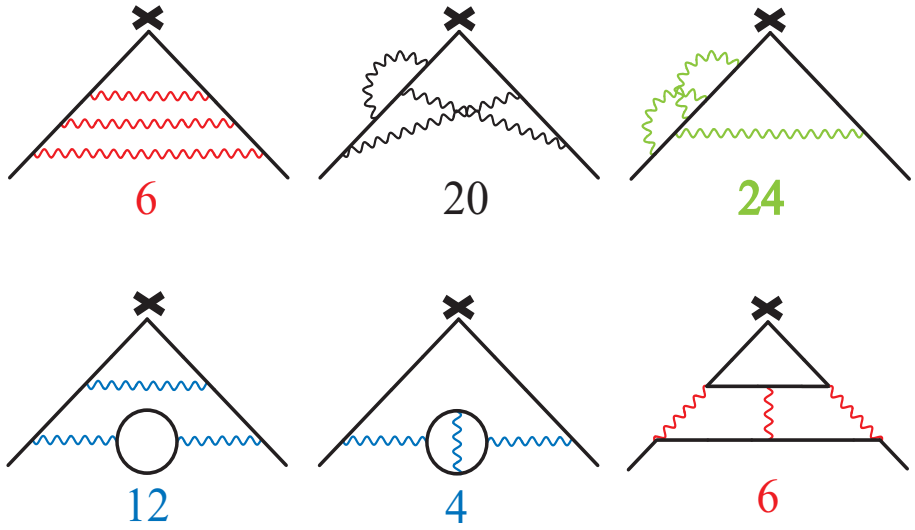

Figure 3: The 72 Feynman diagrams which make up the coefficient A_3 in Eq. (2.21).

The calculation was completed [49] in 1996, with the analytical evaluation of a last class of diagrams, the non planar "triple cross" topologies. The result reads [8]

$$\begin{aligned} A_3 &= \frac{87}{72}\pi^2\zeta(3) - \frac{215}{24}\zeta(5) + \frac{100}{3}\left[\left(a_4 + \frac{1}{24}\ln^4 2\right) - \frac{1}{24}\pi^2\ln^2 2\right] \\ &\quad - \frac{239}{2160}\pi^4 + \frac{139}{18}\zeta(3) - \frac{298}{9}\pi^2\ln 2 + \frac{17101}{810}\pi^2 + \frac{28259}{5184} \\ &= 1.181\,241\,456... \end{aligned} \tag{4.8}$$

[7] Actually, the experimental result of Ref. [25] disagreed with the value $A_2 = -2.973$ obtained in [43], and prompted theoreticians to reconsider the calculation. The result obtained by the authors of Refs. [44, 45, 46] reconciled theory with experiment.

[8] The completion of this three-loop program can be followed through Refs. [50]-[55] and [49]. A description of the technical aspects related to this work and an account of its status up to 1990, with references to the corresponding literature, are given in Ref. [56].

where [9] $a_p = \sum_{n=1}^{\infty} \frac{1}{2^n n^p}$. The numerical value extracted from the exact analytical expression given above can be improved to any desired order of precision.

In parallel to these analytical calculations, numerical methods for the evaluation of the higher order contributions were also developed, in particular by Kinoshita and his collaborators (for details, see [57]). The numerical evaluation of the full set of three loop diagrams was achieved in several steps [58]-[64]. The value quoted in [64] is $A_3 = 1.195(26)$, where the error comes from the numerical procedure. In comparison, let us quote the value [65, 57] $A_3 = 1.176\,11\,(42)$ obtained if only a subset of 21 three loop diagrams out of the original set of 72 is evaluated numerically, relying on the analytical results for the remaining 51 ones, and recall the value $A_3 = 1.181\,241\,456...$ obtained from the full analytical evaluation. The error induced on a_e due to the numerical uncertainty in the second, more accurate, value is still $\Delta(a_e) = 5.3 \times 10^{-12}$, whereas the experimental error is only $\Delta(a_e)|_{\rm exp} = 4.3 \times 10^{-12}$. This discussion shows that the analytical evaluations of higher loop contributions to the anomalous magnetic moment of the electron have a strong practical interest as far as the precision of the theoretical prediction is concerned, and which goes well beyond the mere intellectual satisfaction and technical skills involved in these calculations. [10]

At the four loop level, there are 891 diagrams to consider. Clearly, only a few of them have been evaluated analytically [66, 67]. The complete numerical evaluation of the whole set gave [65] $A_4 = -1.434(138)$. The development of computers allowed subsequent reanalyzes to be more accurate, i.e. $A_4 = -1.557(70)$ [68], while the "latest of [these] constantly improving values" is [4]

$$A_4 \,=\, -1.509\,8(38\,4)\,. \tag{4.9}$$

Needless to say, so far the five loop contribution A_5 is unknown territory. On the other hand, $(\alpha/\pi)^5 \sim 7 \times 10^{-14}$, so that one may reasonably expect that, in view of the present experimental situation, its knowledge is not yet required.

4.3 Mass dependent QED corrections

We now turn to the QED loop contributions to the electron's anomalous magnetic moment involving the heavier leptons, μ and τ. The lowest order contribution of this type occurs at the two loop level, $\mathcal{O}(\alpha^2)$, and corresponds to a heavy lepton vacuum polarization insertion in the one loop vertex graph, cf. Fig. 4. Quite generally, the contribution to a_ℓ arising from the insertion, into the one loop vertex correction, of a vacuum polarization graph due to a loop of lepton ℓ', reads [69, 70] [11]

$$B_2(\ell,\ell') \,=\, \frac{1}{3}\int_{4m_{\ell'}^2}^{\infty} dt \sqrt{1-\frac{4m_{\ell'}^2}{t}}\,\frac{t+2m_{\ell'}^2}{t^2}\int_0^1 dx\,\frac{x^2(1-x)}{x^2+(1-x)\,\frac{t}{m_\ell^2}}\,. \tag{4.10}$$

If $m_{\ell'} \gg m_\ell$, the second integrand can be approximated by $x^2 m_\ell^2/t$, and one obtains [72]

$$B_2(\ell,\ell') \,=\, \frac{1}{45}\left(\frac{m_\ell}{m_{\ell'}}\right)^2 + \mathcal{O}\left[\left(\frac{m_\ell}{m_{\ell'}}\right)^3\right]\,,\ m_{\ell'} \gg m_\ell\,. \tag{4.11}$$

[9] The first three values are known to be $a_1 = \ln 2$, $a_2 = {\rm Li}_2(1/2) = (\zeta(2) - \ln^2 2)/2$, $a_3 = \frac{7}{8}\zeta(3) - \frac{1}{2}\zeta(2)\ln 2 + \frac{1}{6}\ln^3 2$ [56].

[10] It is only fair to point out that the numerical values that are quoted here correspond to those given in the original references. It is to be expected that they would improve if today's numerical possibilities were used.

[11] A trivial change of variable on t brings the expression (4.10) into the form given in [69, 70]. Furthermore, the analytical result obtained upon performing the double integration is available in [71].

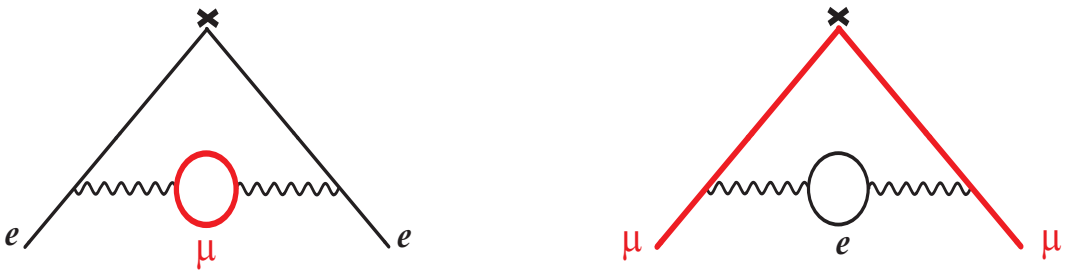

Figure 4: The insertion of a muon vacuum polarization loop into the electron vertex correction (left) or of an electron vacuum polarization loop into the muon vertex correction (right).

Numerically, this translates into [3] [$m_e = 0.51099907(15)$ MeV, $m_\mu/m_e = 206.768273(24)$, $m_\tau = 1\,777.05(26)$]

$$\begin{aligned} B_2(e,\mu) &= 5.197 \times 10^{-7} \\ B_2(e,\tau) &= 1.838 \times 10^{-9}\,. \end{aligned} \tag{4.12}$$

For later use, it is interesting to briefly discuss the structure of Eq. (4.10). The quantity which appears under the integral is related to the cross section for the scattering of a $\ell^+\ell^-$ pair into a pair $(\ell')^+(\ell')^-$ *at lowest order in QED*,

$$\sigma_{QED}^{(\ell^+\ell^-\to(\ell')^+(\ell')^-)}(s) = \frac{4\pi\alpha^2}{3s^2}\sqrt{1-\frac{4m_{\ell'}^2}{s}}\,(s+2m_{\ell'}^2)\,, \tag{4.13}$$

so that

$$B_2(\ell;\ell') = \frac{1}{3}\int_{4m_{\ell'}^2} dt K(t) R^{(\ell')}(t)\,, \tag{4.14}$$

where

$$K(t) = \int_0^1 dx\,\frac{x^2(1-x)}{x^2+(1-x)\,\frac{t}{m_\ell^2}}\,, \tag{4.15}$$

and $R^{(\ell')}(t)$ is the *lowest order* QED cross section $\sigma_{QED}^{(\ell^+\ell^-\to(\ell')^+(\ell')^-)}(s)$ divided by the asymptotic form of the cross section of the reaction $e^+e^-\to\mu^+\mu^-$ for $s \gg m_\mu^2$, $\sigma_\infty^{(e^+e^-\to\mu^+\mu^-)}(s) = \frac{4\pi\alpha^2}{3s}$.

The three loop contributions with different lepton flavours in the loops are also known analytically [73, 74]. It is convenient to distinguish three classes of diagrams. The first group contains all the diagrams with one or two vacuum polarization insertion involving the same lepton, μ or τ, of the type shown in Fig. 5. The second group consists of the leptonic light-by-light scattering insertion diagrams, Fig. 6. Finally, since there are three flavours of massive leptons in the standard model, one has also the possibility of having graphs with two heavy lepton vacuum polarization insertions, one made of a muon loop, the other of a τ loop. This gives

$$B_3(e,\ell) = B_3^{(\mathrm{v.p.})}(e;\mu) + B_3^{(\mathrm{v.p.})}(e;\tau) + B_3^{(\mathrm{L\times L})}(e;\mu) + B_3^{(\mathrm{L\times L})}(e;\tau) + B_3^{(\mathrm{v.p.})}(e;\mu,\tau)\,. \tag{4.16}$$

The analytical expression for $B_3^{(\mathrm{v.p.})}(e;\mu)$ can be found in Ref. [73], whereas [74] gives the corresponding result for $B_3^{(\mathrm{L\times L})}(e;\mu)$. For practical purposes, it is both sufficient and more convenient to use their expansions in powers of m_e/m_μ,

$$B_3^{(\mathrm{v.p.})}(e;\mu) = \left(\frac{m_e}{m_\mu}\right)^2\left[-\frac{23}{135}\ln\left(\frac{m_\mu}{m_e}\right) - \frac{2}{45}\pi^2 + \frac{10117}{24300}\right]$$

$$
\begin{aligned}
&+ \quad \left(\frac{m_e}{m_\mu}\right)^4 \left[\frac{19}{2520}\ln^2\left(\frac{m_\mu}{m_e}\right) - \frac{14233}{132300}\ln\left(\frac{m_\mu}{m_e}\right) + \frac{49}{768}\zeta(3) - \frac{11}{945}\pi^2 + \frac{2976691}{296352000}\right] \\
&+ \quad \mathcal{O}\left[\left(\frac{m_e}{m_\mu}\right)^6\right] \\
&= \quad -0.000\,021\,768... \qquad (4.17)
\end{aligned}
$$

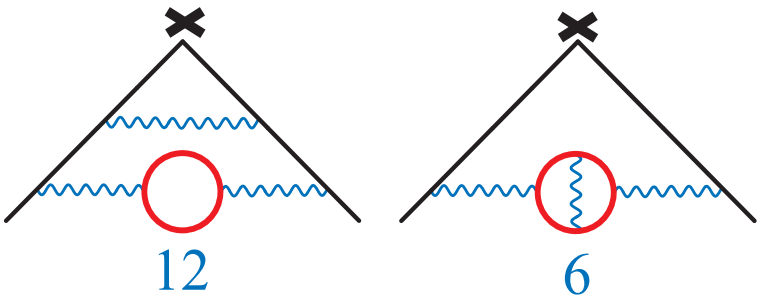

Figure 5: Three loop QED corrections with insertion of a heavy lepton vacuum polarization which make up the coefficient $B_3^{(\mathrm{v.p.})}(e;\mu)$.

and [74]

$$
\begin{aligned}
B_3^{(\mathrm{L\times L})}(e;\mu) &= \left(\frac{m_e}{m_\mu}\right)^2 \left[\frac{3}{2}\zeta(3) - \frac{19}{16}\right] \\
&+ \left(\frac{m_e}{m_\mu}\right)^4 \left[-\frac{161}{810}\ln^2\left(\frac{m_\mu}{m_e}\right) - \frac{16189}{48600}\ln\left(\frac{m_\mu}{m_e}\right) + \frac{13}{18}\zeta(3) - \frac{161}{9720}\pi^2 - \frac{831931}{972000}\right] \\
&+ \mathcal{O}\left[\left(\frac{m_e}{m_\mu}\right)^6\right] \\
&= 0.000\,014\,394\,5... \qquad (4.18)
\end{aligned}
$$

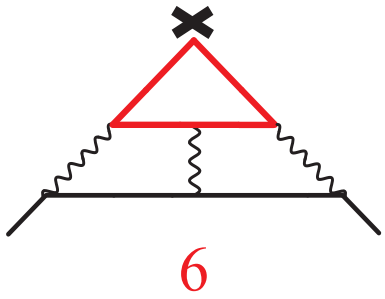

Figure 6: The three loop QED correction with the insertion of a heavy lepton light-by-light scattering subgraph, corresponding to the coefficient $B_3^{(\mathrm{L\times L})}(e;\mu)$.

The expressions for $B_3^{(\mathrm{v.p.})}(e;\tau)$ and $B_3^{(\mathrm{L\times L})}(e;\tau)$ follow upon replacing the muon mass m_μ by m_τ. This again gives a suppression factor $(m_\mu/m_\tau)^2$, which makes these contributions negligible at the present level of precision. For the same reason, $B_3^{(\mathrm{v.p.})}(e;\mu,\tau)$ can also be discarded.

4.4 Other contributions to a_e

In order to make the discussion of the standard model contributions to a_e complete, there remains to mention the hadronic and weak components, $a_e^{\rm had}$ and $a_e^{\rm weak}$, respectively. Their features will be discussed in detail below, in the context of the anomalous magnetic moment of the muon. I therefore only quote the numerical values [12]

$$a_e^{\rm had} \;=\; 1.67(3)\times 10^{-12}\,, \tag{4.19}$$

and [75]

$$a_e^{\rm weak} \;=\; 0.030\times 10^{-12} \tag{4.20}$$

4.5 Comparison with experiment and determination of α

Summing up the various contributions discussed so far gives the standard model prediction [3, 4, 7]

$$a_e^{\rm SM} \;=\; 0.5\,\frac{\alpha}{\pi} - 0.328\,478\,444\,00\left(\frac{\alpha}{\pi}\right)^2 + 1.181\,234\,017\left(\frac{\alpha}{\pi}\right)^3 - 1.509\,8(38\,4)\left(\frac{\alpha}{\pi}\right)^4 + 1.70\times 10^{-12}\,. \tag{4.21}$$

In order to obtain a number that can be compared to the experimental result, a sufficiently accurate determination of the fine structure constant α is required. The best available measurement of the latter comes from the quantum Hall effect [76],

$$\alpha^{-1}(qH) \;=\; 137.036\,003\,00(2\,70) \tag{4.22}$$

and leads to

$$a_e^{\rm SM}(qH) \;=\; 0.001\,159\,652\,153\,5(24\,0)\,, \tag{4.23}$$

about six times less accurate than the latest experimental value [21]

$$a_e^{\rm exp} \;=\; 0.001\,159\,652\,188\,4(4\,3)\,. \tag{4.24}$$

On the other hand, if one excludes other contributions to a_e than those from the standard model considered so far, and believes that all theoretical errors are under control, then the above value of $a_e^{\rm exp}$ provides the best determination of α to date,

$$\alpha^{-1}(a_e) \;=\; 137.035\,999\,58(52)\,. \tag{4.25}$$

5 The anomalous magnetic moment of the muon

In this section, we discuss the theoretical aspects concerning the anomalous magnetic moment of the muon. Since the muon is much heavier than the electron, a_μ will be more sensitive to higher mass scales. In particular, it is a better probe for possible degrees of freedom beyond the standard model, like supersymmetry. The drawback, however, is that a_μ will also be more sensitive to the non perturbative strong interaction dynamics at the ~ 1 GeV scale.

[12] I reproduce here the values given in [3, 4], except for the fact that I have taken into account the changes in the value of the hadronic light-by-light contribution to a_μ, see below, for which I take $a_\mu^{(\rm L\times L)} = +8(4)\times 10^{-10}$, and which translates into $a_e^{(\rm L\times L)} \sim a_\mu^{(\rm L\times L)}(m_e/m_\mu)^2 = 0.02\times 10^{-12}$.

5.1 QED contributions to a_μ

As already mentioned before, the mass independent QED contributions to a_μ are described by the same coefficients A_n as in the case of the electron. We therefore need only to discuss the coefficients $B_n(\mu;\ell')$ associated with the mass dependent corrections.

For $m_{\ell'} \ll m_\ell$, Eq. (4.10) gives [69, 70, 71]

$$B_2(\ell;\ell') \,=\, \frac{1}{3}\,\ln\left(\frac{m_\ell}{m_{\ell'}}\right) - \frac{25}{36} + \frac{3}{2}\frac{m_\ell}{m_{\ell'}}\zeta(2) - 4\left(\frac{m_\ell}{m_{\ell'}}\right)^2 \ln\left(\frac{m_\ell}{m_{\ell'}}\right) + 3\left(\frac{m_\ell}{m_{\ell'}}\right)^2 + \mathcal{O}\left[\left(\frac{m_\ell}{m_{\ell'}}\right)^3\right], \tag{5.1}$$

which translates into the numerical values [3]

$$B_2(\mu;e) \,=\, 1.094\,258\,294(37) \tag{5.2}$$

$$B_2(\mu;\tau) \,=\, 0.00\,078\,059(23)\,. \tag{5.3}$$

Although these numbers follow from an analytical expression, there are uncertainties attached to them, induced by those on the corresponding values of the ratios of the lepton masses.

The three loop QED corrections decompose as

$$B_3(\mu,\ell) \,=\, B_3^{(\mathrm{v.p.})}(\mu;e) \,+\, B_3^{(\mathrm{v.p.})}(\mu;\tau) \,+\, B_3^{(\mathrm{L\times L})}(\mu;e) \,+\, B_3^{(\mathrm{L\times L})}(\mu;\tau) \,+\, B_3^{(\mathrm{v.p.})}(\mu;e,\tau)\,. \tag{5.4}$$

with [73, 74]

$$\begin{aligned}
B_3^{(\mathrm{v.p.})}(\mu;e) \,=\, & \frac{2}{9}\,\ln^2\left(\frac{m_\mu}{m_e}\right) \,+\, \left[\zeta(3) - \frac{2}{3}\pi^2\ln 2 + \frac{1}{9}\pi^2 + \frac{31}{27}\right]\ln\left(\frac{m_\mu}{m_e}\right) \\
& + \frac{11}{216}\pi^4 \,-\, \frac{2}{9}\pi^2\ln^2 2 \,-\, \frac{8}{3}a_4 \,-\, \frac{1}{9}\ln^4 2 \,-\, 3\zeta(3) \,+\, \frac{5}{3}\pi^2\ln 2 \,-\, \frac{25}{18}\pi^2 \,+\, \frac{1075}{216} \\
& + \frac{m_e}{m_\mu}\left[-\frac{13}{18}\pi^3 - \frac{16}{9}\pi^2\ln 2 + \frac{3199}{1080}\pi^2\right] \\
& + \left(\frac{m_e}{m_\mu}\right)^2\left[\frac{10}{3}\ln^2\left(\frac{m_\mu}{m_e}\right) - \frac{11}{9}\ln\left(\frac{m_\mu}{m_e}\right) - \frac{14}{3}\pi^2\ln 2 - 2\zeta(3) + \frac{49}{12}\pi^2 - \frac{131}{54}\right] \\
& + \left(\frac{m_e}{m_\mu}\right)^3\left[\frac{4}{3}\pi^2\ln\left(\frac{m_\mu}{m_e}\right) + \frac{35}{12}\pi^3 - \frac{16}{3}\pi^2\ln 2 - \frac{5771}{1080}\pi^2\right] \\
& + \left(\frac{m_e}{m_\mu}\right)^4\left[-\frac{25}{9}\ln^3\left(\frac{m_\mu}{m_e}\right) - \frac{1369}{180}\ln^2\left(\frac{m_\mu}{m_e}\right)\right. \\
& \left. + [-2\zeta(3) + 4\pi^2\ln 2 - \frac{269}{144}\pi^2 - \frac{7496}{675}]\ln\left(\frac{m_\mu}{m_e}\right)\right. \\
& \left. - \frac{43}{108}\pi^4 \,+\, \frac{8}{9}\pi^2\ln^2 2 \,+\, \frac{80}{3}a_4 \,+\, \frac{10}{9}\ln^4 2 \,-\, \frac{411}{32}\zeta(3) \,+\, \frac{89}{48}\pi^2\ln 2 \,-\, \frac{1061}{864}\pi^2 \,-\, \frac{274511}{54000}\right] \\
& + \mathcal{O}\left[\left(\frac{m_e}{m_\mu}\right)^5\right],
\end{aligned} \tag{5.5}$$

$$\begin{aligned}
B_3^{(\mathrm{L\times L})}(\mu;e) \,=\, & \frac{2}{3}\,\pi^2\,\ln\left(\frac{m_\mu}{m_e}\right) \,+\, \frac{59}{270}\,\pi^4 \,-\, 3\zeta(3) \,-\, \frac{10}{3}\,\pi^2 \,+\, \frac{2}{3} \\
& + \frac{m_e}{m_\mu}\left[\frac{4}{3}\pi^2\ln\left(\frac{m_\mu}{m_e}\right) - \frac{196}{3}\pi^2\ln 2 + \frac{424}{9}\pi^2\right] \\
& + \left(\frac{m_e}{m_\mu}\right)^2\left[-\frac{2}{3}\ln^3\left(\frac{m_\mu}{m_e}\right) + (\frac{\pi^2}{9} - \frac{20}{3})\ln^2\left(\frac{m_\mu}{m_e}\right) - [\frac{16}{135}\pi^4 + 4\zeta(3) - \frac{32}{9}\pi^2 + \frac{61}{3}]\ln\left(\frac{m_\mu}{m_e}\right)\right.
\end{aligned}$$

$$+\frac{4}{3}\zeta(3)\pi^2 - \frac{61}{270}\pi^4 + 3\zeta(3) + \frac{25}{18}\pi^2 - \frac{283}{12}\Bigg]$$
$$+ \left(\frac{m_e}{m_\mu}\right)^3 \left[\frac{10}{9}\pi^2 \ln\left(\frac{m_\mu}{m_e}\right) - \frac{11}{9}\pi^2\right]$$
$$+ \left(\frac{m_e}{m_\mu}\right)^4 \left[\frac{7}{9}\ln^3\left(\frac{m_\mu}{m_e}\right) + \frac{41}{18}\ln^2\left(\frac{m_\mu}{m_e}\right) + \frac{13}{9}\pi^2 \ln\left(\frac{m_\mu}{m_e}\right) + \frac{517}{108}\ln\left(\frac{m_\mu}{m_e}\right)\right.$$
$$\left. +\frac{1}{2}\zeta(3) + \frac{191}{216}\pi^2 + \frac{13283}{2592}\right] + \mathcal{O}\left[\left(\frac{m_e}{m_\mu}\right)^5\right], \tag{5.6}$$

while $B_3^{(\mathrm{v.p.})}(\mu;\tau)$ and $B_3^{(\mathrm{L\times L})}(\mu;\tau)$ are derived from $B_3^{(\mathrm{v.p.})}(\mu;\tau)$ and from $B_3^{(\mathrm{L\times L})}(\mu;\tau)$, respectively, by trivial substitutions of the masses. Furthermore, the graphs with mixed vacuum polarization insertions, one electron loop, and one τ loop, are evaluated numerically using a dispersive integral [51, 73, 77].

Numerically, one obtains (we quote here the numerical values updated in [3])

$$\begin{aligned}
B_3^{(\mathrm{v.p.})}(\mu;e) &= 1.920\,455\,1(2)\\
B_3^{(\mathrm{L\times L})}(\mu;e) &= 20.947\,924\,6(7)\\
B_3^{(\mathrm{v.p.})}(\mu;\tau) &= -0.001\,782\,2(4)\\
B_3^{(\mathrm{L\times L})}(\mu;\tau) &= 0.002\,142\,8(7)\\
B_3^{(\mathrm{v.p.})}(\mu;e,\tau) &= 0.000\,527\,6(2)\,.
\end{aligned} \tag{5.7}$$

Notice the large value of $B_3^{(\mathrm{L\times L})}(\mu;e)$, due to the occurrence of terms involving factors like $\ln(m_\mu/m_e) \sim 5$ and powers of π.

5.2 Hadronic contributions to a_μ

On the level of Feynman diagrams, hadronic contributions arise through loops of virtual quarks and gluons. These loops also involve the soft scales, and therefore cannot be computed reliably in perturbative QCD. We shall decompose the hadronic contributions into three subsets: hadronic vacuum polarization insertions at order α^2, at order α^3, and hadronic light-by-light scattering,

$$a_\mu^{\mathrm{had}} = a_\mu^{(\mathrm{h.v.p.\ 1})} + a_\mu^{(\mathrm{h.v.p.\ 2})} + a_\mu^{(\mathrm{h.\ L\times L})} \tag{5.8}$$

5.2.1 Hadronic vacuum polarization

We first discuss $a_\mu^{(\mathrm{h.v.p.\ 1})}$, which arises at order $\mathcal{O}(\alpha^2)$ from the insertion of a single hadronic vacuum polarization into the lowest order vertex correction graph, see Fig. 7. The importance of this contribution to a_μ is known since long time [78, 79].

There is a very convenient dispersive representation of this diagram, similar to Eq. (4.10)

$$\begin{aligned}
a_\mu^{(\mathrm{h.v.p.\ 1})} &= \frac{\alpha}{\pi}\int_{4M_\pi^2}^{\infty}\frac{dt}{t}\,K(t)\,\frac{1}{\pi}\,\mathrm{Im}\Pi(t)\\
&= \frac{1}{3}\left(\frac{\alpha}{\pi}\right)^2\int_{4M_\pi^2}^{\infty}\frac{dt}{t}\,K(t)R^{\mathrm{had}}(t)\,,
\end{aligned} \tag{5.9}$$

Here, $\Pi(t)$ denotes the *hadronic* component of the vacuum polarization function, defined as [13]

$$(q_\mu q_\nu - q^2\eta_{\mu\nu})\Pi(Q^2) = i\int d^4x e^{iq\cdot x}\,\langle\Omega|\mathrm{T}\{j_\mu(x)j_\nu(0)\}|\Omega\rangle\,, \tag{5.10}$$

[13] Actually, $\Pi(t)$ defined this way has an ultraviolet divergence, produced by the QCD short distance singularity of the chronological product of the two currents. However, it only affects the real part of $\Pi(t)$. A renormalized, finite quantity is obtained by a single subtraction, $\Pi(t) - \Pi(0)$.

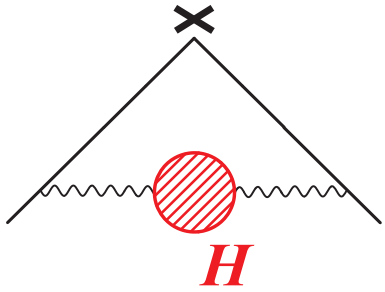

Figure 7: The insertion of the hadronic vacuum polarization into the one loop vertex correction, corresponding to $a_\mu^{(\text{h.v.p. 1})}$.

with j_ρ the hadronic component of the electromagnetic current, $Q^2 = -q^2 \geq 0$ for q_μ spacelike, and $|\Omega\rangle$ the QCD vacuum. The function $K(t)$ was defined in Eq. (4.15), and $R^{\text{had}}(t)$ stands now for the cross section of $e^+e^- \to$ hadrons, *at lowest order in* α, divided by $\sigma_\infty^{(e^+e^-\to\mu^+\mu^-)}(s) = \frac{4\pi\alpha^2}{3s}$. A first principle computation of this strong interaction contribution is far beyond our present abilities to deal with the non perturbative aspects of confining gauge theories. This last relation is however very interesting because it expresses $a_\mu^{(\text{h.v.p. 1})}$ through a quantity that can be measured experimentally. In this respect, two important properties of the function $K(t)$ deserve to be mentioned. First, it appears from the integral representation (4.15) that $K(t)$ is positive definite. Since $R_{e^+e^-}$ is also positive, one deduces that $a_\mu^{(\text{h.v.p. 1})}$ itself is positive. Second, the function $K(t)$ decreases as $m_\mu^2/3t$ as t grows, so that it is indeed the low energy region which dominates the integral. Explicit evaluation of $a_\mu^{(\text{h.v.p. 1})}$ using available data actually reveals that more than 80% of its value comes from energies below 1.4 GeV. Finally, the values obtained this way for $a_\mu^{(\text{h.v.p. 1})}$ have evolved in time, as shown in Table 3. This evolution is mainly driven by the availability of more data, and is still going on, as the last entries of Table 3 show. In order to match the precision reached by the latest experimental measurement of a_μ, $a_\mu^{(\text{h.v.p. 1})}$ needs to be known at $\sim 1\%$. Besides the very recent high quality e^+e^- data obtained by the BES Collaboration [80] in the region between 2 to 5 GeV, and by the CMD-2 collaboration [81] in the region dominated by the ρ resonance, the latest analyses sometimes also include or use, in the low-energy region, data obtained from hadronic decays of the τ by ALEPH [82], and, more recently, by CLEO [83]. We may notice from Table 3 that the precision obtained by using e^+e^- data alone has become comparable to the one achieved upon including the τ data. However, one of the latest analyses reveals a troubling discrepancy between the e^+e^- and τ evaluations. Additional work is certainly needed in order to resolve these problems. Further data are also expected in the future, from the KLOE experiment at the DAPHNE e^+e^- machine, or from the B factories BaBar and Belle. For additional comparative discussions and details of the various analyses, we refer the reader to the literature quoted in Table 3.

Let us briefly mention here that it is quite easy to estimate the order of magnitude of $a_\mu^{(\text{h.v.p. 1})}$. For this purpose, it is convenient to introduce still another representation [93], which relates $a_\mu^{(\text{h.v.p. 1})}$ to the hadronic Adler function $\mathcal{A}(Q^2)$, defined as [14]

$$\mathcal{A}(Q^2) \;=\; -Q^2\,\frac{\partial\Pi(Q^2)}{\partial Q^2} \;=\; \int_0^\infty dt\,\frac{Q^2}{(t+Q^2)^2}\,\frac{1}{\pi}\,\text{Im}\Pi(t)\,, \tag{5.11}$$

by

$$a_\mu^{(\text{h.v.p. 1})} \;=\; 2\pi^2\,\left(\frac{\alpha}{\pi}\right)^2\,\int_0^1 \frac{dx}{x}(1-x)(2-x)\mathcal{A}\left(\frac{x^2}{1-x}\,m_\mu^2\right)\,. \tag{5.12}$$

[14] Unlike $\Pi(t)$ itself, $\mathcal{A}(Q^2)$ if free from ultraviolet divergences.

Table 3: Some of the recent evaluations of $a_\mu^{(\mathrm{h.v.p.\ 1})} \times 10^{-11}$ from e^+e^- and/or τ-decay data.

7024(153)	[84]	e^+e^-
7026(160)	[85]	e^+e^-
6950(150)	[86]	e^+e^-
7011(94)	[86]	τ, e^+e^-,
6951(75)	[87]	τ, e^+e^-, QCD
6924(62)	[88]	τ, e^+e^-, QCD
	[89]	QCD sum rules
7036(76)	[41]	τ, e^+e^-, QCD
7002(73)	[90]	e^+e^-, F_π
6974(105)	[91]	e^+e^-, incl. BES-II data
6847(70)	[92]	e^+e^-, incl. BES-II and CMD-2 data
7019(62)	[92]	τ, e^+e^-
6831(62)	[94]	e^+e^-

A simple representation of the hadronic Adler function can be obtained if one assumes that $\mathrm{Im}\Pi(t)$ is given by a single, zero width, vector meson pole, and, above a certain threshold s_0, by the QCD perturbative continuum contribution,

$$\frac{1}{\pi}\,\mathrm{Im}\Pi(t) \;=\; \frac{2}{3}\,f_V^2 M_V^2\,\delta(t-M_V^2) \;+\; \frac{2}{3}\,\frac{N_C}{12\pi^2}\,\left[1+\mathcal{O}(\alpha_s)\right]\,\theta(t-s_0) \tag{5.13}$$

The justification [95] for this type of minimal hadronic ansatz can be found within the framework of the large-N_C limit [96, 97] of QCD, see Ref. [95] for a general discussion and a detailed study of this representation of the Adler function. The threshold s_0 for the onset of the continuum can be fixed from the property that there is no contribution in $1/Q^2$ in the short distance expansion of $\mathcal{A}(Q^2)$, which requires [95]

$$2f_V^2 M_V^2 \;=\; \frac{N_C}{12\pi^2}\,s_0\,\left(1\;+\;\frac{3}{8}\,\frac{\alpha_s(s_0)}{\pi}\;+\;\mathcal{O}(\alpha_s^2)\right)\,. \tag{5.14}$$

This then gives [98] $a_\mu^{(\mathrm{h.v.p.\ 1})} \sim (570 \pm 170) \times 10^{-10}$, which compares well with the more elaborate data based evaluations in Table 3, even though this simple estimate cannot claim to provide the required accuracy of about 1%.

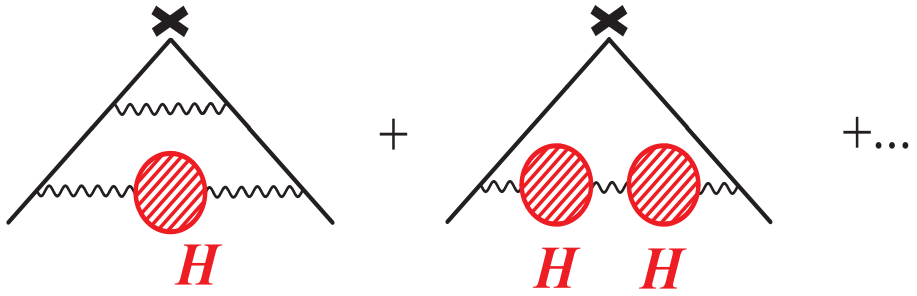

Figure 8: Higher order corrections containing the hadronic vacuum polarization contribution, corresponding to $a_\mu^{(\mathrm{h.v.p.\ 2})}$.

We now come to the $\mathcal{O}(\alpha^3)$ corrections involving hadronic vacuum polarization subgraphs. Besides the contributions shown in Fig. 8, another one is obtained upon inserting a lepton loop in one of the two photon lines of the graph shown in Fig. 7. These can again be expressed in terms of $R^{\rm had}$ [99, 2, 77]

$$a_\mu^{(\rm h.v.p.\ 2)} \;=\; \frac{1}{3}\,\left(\frac{\alpha}{\pi}\right)^3 \int_{4M_\pi^2}^\infty \frac{dt}{t}\,K^{(2)}(t)R^{\rm had}(t)\,. \tag{5.15}$$

Unlike $K(t)$, the function $K^{(2)}(t)$ is not positive definite, so that the sign of $a_\mu^{(\rm h.v.p.\ 2)}$ is not fixed on the basis of general considerations. The value obtained for this quantity is [77] $a_\mu^{(\rm h.v.p.\ 2)}\times 10^{11} = -101\pm 6$.

5.2.2 Hadronic light-by-light scattering

We now discuss the so called hadronic light-by-light scattering graphs of Fig. 9. Actually, there is another $\mathcal{O}(\alpha^3)$ correction involving the amplitude for virtual light-by-light scattering, namely the one obtained by adding an additional photon line attached to the hadronic blob in Fig. 7. This contribution is usually included in the evaluations reported on in Table 3 [see the discussion in [92]], otherwise, it has been added. The reason for that is due to the fact that the measured e^+e^- data contain QED effects, and do not correspond to the cross section of $e^+e^-\to$ hadrons restricted to the *lowest order* in α. It is possible to compute and subtract away QED corrections involving the leptonic vertex, but there still remain radiative corrections between the final state hadrons, or which affect both the initial and the final states. These cannot be evaluated in a model independent way, and are not completely described by attaching a photon loop to the hadronic blob in Fig. 7.

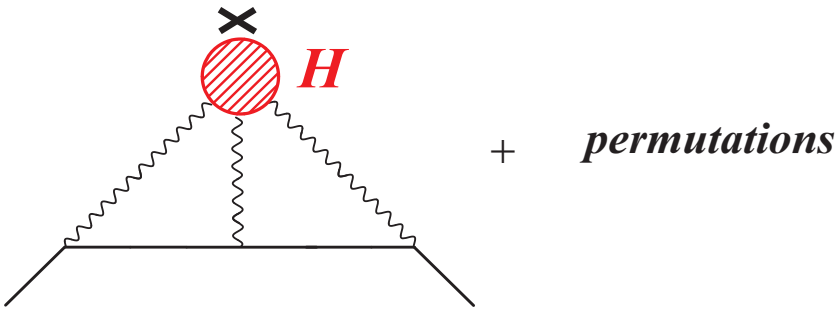

Figure 9: The hadronic light-by-light scattering graphs contributing to $a_\mu^{(\rm h.\ L\times L)}$.

Coming back to the diagram of Fig. 9, the contribution to $\Gamma_\rho(p',p)$ of relevance here is the matrix element, at lowest nonvanishing order in the fine structure constant α, of the light quark electromagnetic current

$$j_\rho(x) \;=\; \frac{2}{3}(\bar u\gamma_\rho u)(x) \;-\; \frac{1}{3}(\bar d\gamma_\rho d)(x) \;-\; \frac{1}{3}(\bar s\gamma_\rho s)(x) \tag{5.16}$$

between μ^- states,

$$\begin{aligned}(-ie)\bar{\rm u}(p')\Gamma_\rho^{(\rm h.\ L\times L)}(p',p){\rm u}(p) \;&\equiv\; \langle\mu^-(p')|(ie)j_\rho(0)|\mu^-(p)\rangle\\ &=\; \int\frac{d^4q_1}{(2\pi)^4}\int\frac{d^4q_2}{(2\pi)^4}\,\frac{(-i)^3}{q_1^2\,q_2^2\,(q_1+q_2-k)^2}\\ &\times\,\frac{i}{(p'-q_1)^2-m^2}\,\frac{i}{(p'-q_1-q_2)^2-m^2}\\ &\times\,(-ie)^3\overline{\rm u}(p')\gamma^\mu(\not p'-\not q_1+m)\gamma^\nu(\not p'-\not q_1-\not q_2+m)\gamma^\lambda{\rm u}(p)\\ &\times\,(ie)^4\Pi_{\mu\nu\lambda\rho}(q_1,q_2,k-q_1-q_2)\,,\end{aligned} \tag{5.17}$$

with $k_\mu = (p' - p)_\mu$ and

$$\Pi_{\mu\nu\lambda\rho}(q_1,q_2,q_3) = \int d^4x_1 \int d^4x_2 \int d^4x_3\, e^{i(q_1\cdot x_1 + q_2\cdot x_2 + q_3\cdot x_3)} \times \langle\, \Omega \,|\, \mathrm{T}\{j_\mu(x_1) j_\nu(x_2) j_\lambda(x_3) j_\rho(0)\} \,|\, \Omega \,\rangle \tag{5.18}$$

the fourth-rank light quark hadronic vacuum-polarization tensor, $|\,\Omega\,\rangle$ denoting the QCD vacuum. Since the flavour diagonal current $j_\mu(x)$ is conserved, the tensor $\Pi_{\mu\nu\lambda\rho}(q_1,q_2,q_3)$ satisfies the Ward identities

$$\{q_1^\mu; q_2^\nu; q_3^\lambda; (q_1+q_2+q_3)^\rho\}\Pi_{\mu\nu\lambda\rho}(q_1,q_2,q_3) \,=\, 0\,. \tag{5.19}$$

This entails that [15]

$$\bar{\mathrm{u}}(p')\Gamma_\rho^{(\mathrm{h.\ L\times L})}(p',p)\mathrm{u}(p) \,=\, \bar{\mathrm{u}}(p')\left[\gamma_\rho F_1^{(\mathrm{h.\ L\times L})}(k^2) \,+\, \frac{i}{2m}\,\sigma_{\rho\tau}k^\tau F_2^{(\mathrm{h.\ L\times L})}(k^2)\right]\mathrm{u}(p)\,, \tag{5.20}$$

as well as $\Gamma_\rho^{(\mathrm{h.\ L\times L})}(p',p) = k^\tau \Gamma_{\rho\tau}^{(\mathrm{h.\ L\times L})}(p',p)$ with

$$\begin{aligned}\bar{\mathrm{u}}(p')\Gamma_{\rho\sigma}^{(\mathrm{h.\ L\times L})}(p',p)\mathrm{u}(p) \;=\; & -ie^6 \int \frac{d^4q_1}{(2\pi)^4}\int \frac{d^4q_2}{(2\pi)^4}\,\frac{1}{q_1^2\,q_2^2\,(q_1+q_2-k)^2} \\ & \times \frac{1}{(p'-q_1)^2-m^2}\,\frac{1}{(p'-q_1-q_2)^2-m^2} \\ & \times \bar{\mathrm{u}}(p')\gamma^\mu(\not{p}'-\not{q}_1+m)\gamma^\nu(\not{p}'-\not{q}_1-\not{q}_2+m)\gamma^\lambda \mathrm{u}(p) \\ & \times \frac{\partial}{\partial k^\rho}\,\Pi_{\mu\nu\lambda\sigma}(q_1,q_2,k-q_1-q_2)\,.\end{aligned} \tag{5.21}$$

Following Ref. [58] and using the property $k^\rho k^\sigma \bar{\mathrm{u}}(p')\Gamma_{\rho\sigma}^{(\mathrm{h.\ L\times L})}(p',p)\mathrm{u}(p) = 0$, one deduces that $F_1^{(\mathrm{h.\ L\times L})}(0) = 0$ and that the hadronic light-by-light contribution to the muon anomalous magnetic moment is equal to

$$a_\mu^{(\mathrm{h.\ L\times L})} \,\equiv\, F_2^{(\mathrm{h.\ L\times L})}(0) \,=\, \frac{1}{48m}\,\mathrm{tr}\left\{(\not{p}+m)[\gamma^\rho,\gamma^\sigma](\not{p}+m)\Gamma_{\rho\sigma}^{(\mathrm{h.\ L\times L})}(p,p)\right\}\,. \tag{5.22}$$

This is about all we can say about the QCD four-point function $\Pi_{\mu\nu\lambda\rho}(q_1,q_2,q_3)$. Unlike the hadronic vacuum polarization function, there is no experimental data which would allow for an evaluation of $a_\mu^{(\mathrm{h.\ L\times L})}$. The existing estimates regarding this quantity therefore rely on specific models in order to account for the non perturbative QCD aspects. A few particular contributions can be identified, see Fig. 10. For instance, there is a contribution where the four photon lines are attached to a closed loop of charged mesons. The case of the charged pion loop with pointlike couplings is actually finite and contributes $\sim 4\times 10^{-10}$ to a_μ [100]. If the coupling of charged pions to photons is modified by taking into account the effects of resonances like the ρ, this contribution is reduced by a factor varying between 3 [100, 102] and 10 [101], depending on the resonance model used. Another class of contributions consists of those involving resonance exchanges between photon pairs [100, 101, 102, 103]. Although here also the results depend on the models used, there is a constant feature that emerges from all the analyses that have been done: the contribution coming from the exchange of the pseudoscalars, π^0, η and η' gives practically the final result. Other contributions [charged pion loops, vector, scalar, and axial resonances,...] tend to cancel among themselves.

Some of the results obtained for $a_\mu^{(\mathrm{h.\ L\times L})}\times 10^{-11}$ have been gathered in Table 4. Leaving aside the first result [99, 2] shown there, which is affected by a bad numerical convergence [100], one notices that the sign of this contribution has changed twice. The first change resulted from a mistake

[15] We use the following conventions for Dirac's γ-matrices: $\{\gamma_\mu,\gamma_\nu\} = 2\eta_{\mu\nu}$, with $\eta_{\mu\nu}$ the flat Minkowski space metric of signature $(+---)$, $\sigma_{\mu\nu} = (i/2)[\gamma_\mu,\gamma_\nu]$, $\gamma_5 = i\gamma^0\gamma^1\gamma^2\gamma^3$, whereas the totally antisymmetric tensor $\varepsilon_{\mu\nu\rho\sigma}$ is chosen such that $\varepsilon_{0123} = +1$.

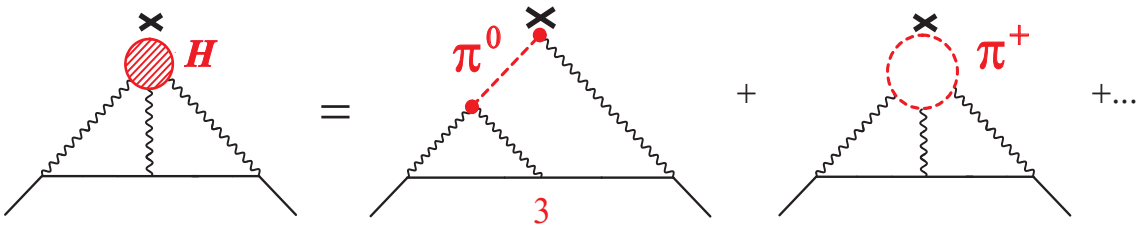

Figure 10: Some individual contributions to hadronic light-by-light scattering: the neutral pion pole and the charged pion loop. There are other contributions, not shown here.

in Ref. [100], that was corrected for in [101]. The minus sign that resulted was confirmed by an independent calculation, using the ENJL model, in Ref. [102]. A subsequent reanalysis [103] gave additional support to a negative result, while also getting better agreement with the value of Ref. [102].

Table 4: Various evaluations of $a_\mu^{(\text{h. L}\times\text{L})} \times 10^{-11}$ and of the pion pole contribution $a_\mu^{(\text{h. L}\times\text{L};\pi^0)} \times 10^{-11}$.

–260(100)	constituent quark loop	[99, 2]
+60(4)	constituent quark loop	[100]
+49(5)	$\pi^\pm$loop, π^0 and resonance poles, $a_\mu^{(\text{h. L}\times\text{L};\pi^0)} = 65(6)$	[100]
–52(18)	$\pi^\pm$ loop, π^0 and resonance poles, and quark loop $a_\mu^{(\text{h. L}\times\text{L};\pi^0)} = -55.60(3)$	[101]
–92(32)	ENJL, $a_\mu^{(\text{h. L}\times\text{L};\pi^0+\eta+\eta')} = -85(13)$	[102]
–79.2(15.4)	$\pi^\pm$ loop, π^0 pole and quark loop, $a_\mu^{(\text{h. L}\times\text{L};\pi^0)} = -55.60(3)$	[103]
+83(12)	π^0, η and η' poles only	[104]
+89.6(15.4)	$\pi^\pm$ loop, π^0 pole and quark loop, $a_\mu^{(\text{h. L}\times\text{L};\pi^0)} = +55.60(3)$	[105]
+83(32)	ENJL, $a_\mu^{(\text{h. L}\times\text{L};\pi^0+\eta+\eta')} = 85(13)$	[106]

Needless to say, these evaluations are based on heavy numerical work, which has the drawback of making the final results rather opaque to an intuitive understanding of the physics behind them. We [16] therefore decided to improve things on the analytical side, in order to achieve a better understanding of the relevant features that led to the previous results. Taking advantage of the observation that the pion pole contribution $a_\mu^{(\text{h. L}\times\text{L};\pi^0)}$ was found to dominate the final values obtained for $a_\mu^{(\text{h. L}\times\text{L})}$, we concentrated our efforts on that part, that I shall now describe in greater detail. For a detailed account on how the other contributions to $a_\mu^{(\text{h. L}\times\text{L})}$ arise, I refer the reader to the original works [100]-[103].

The contributions to $\Pi_{\mu\nu\lambda\rho}(q_1,q_2,q_3)$ arising from single neutral pion exchanges, see Fig. 11, read

$$\Pi^{(\pi^0)}_{\mu\nu\lambda\rho}(q_1,q_2,q_3) = i\,\frac{\mathcal{F}_{\pi^0\gamma^*\gamma^*}(q_1^2,q_2^2)\;\mathcal{F}_{\pi^0\gamma^*\gamma^*}(q_3^2,(q_1+q_2+q_3)^2)}{(q_1+q_2)^2-M_\pi^2}\,\varepsilon_{\mu\nu\alpha\beta}\,q_1^\alpha q_2^\beta\,\varepsilon_{\lambda\rho\sigma\tau}\,q_3^\sigma\,(q_1+q_2)^\tau$$
$$+i\,\frac{\mathcal{F}_{\pi^0\gamma^*\gamma^*}(q_1^2,(q_1+q_2+q_3)^2)\;\mathcal{F}_{\pi^0\gamma^*\gamma^*}(q_2^2,q_3^2)}{(q_2+q_3)^2-M_\pi^2}\,\varepsilon_{\mu\rho\alpha\beta}\,q_1^\alpha(q_2+q_3)^\beta\,\varepsilon_{\nu\lambda\sigma\tau}\,q_2^\sigma q_3^\tau$$

[16] A. Nyffeler and myself, in Ref. [104].

$$+\,i\,\frac{\mathcal{F}_{\pi^0\gamma^*\gamma^*}(q_1^2,q_3^2)\;\mathcal{F}_{\pi^0\gamma^*\gamma^*}(q_2^2,(q_1+q_2+q_3)^2)}{(q_1+q_3)^2-M_\pi^2}\;\varepsilon_{\mu\lambda\alpha\beta}\,q_1^\alpha q_3^\beta\;\varepsilon_{\nu\rho\sigma\tau}\,q_2^\sigma\,(q_1+q_3)^\tau\;. \tag{5.23}$$

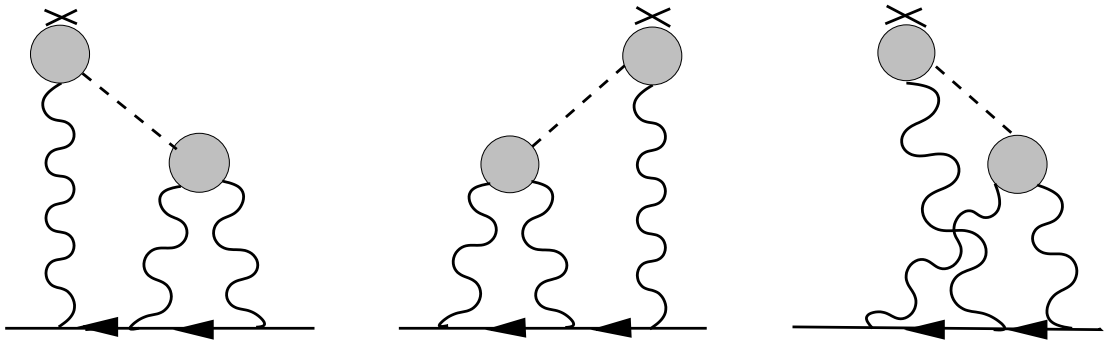

Figure 11: The pion-pole contributions to light-by-light scattering. The shaded blobs represent the form factor $\mathcal{F}_{\pi^0\gamma^*\gamma^*}$. The first and second graphs give rise to identical contributions, involving the function $T_1(q_1,q_2;p)$ in Eq. (5.25), whereas the third graph gives the contribution involving $T_2(q_1,q_2;p)$.

The form factor $\mathcal{F}_{\pi^0\gamma^*\gamma^*}(q_1^2,q_2^2)$, which corresponds to the shaded blobs in Fig. 11, is defined as

$$i\int d^4x e^{iq\cdot x}\langle\,\Omega|T\{j_\mu(x)j_\nu(0)\}|\pi^0(p)\rangle\;=\;\varepsilon_{\mu\nu\alpha\beta}\,q^\alpha p^\beta\,\mathcal{F}_{\pi^0\gamma^*\gamma^*}(q^2,(p-q)^2)\,, \tag{5.24}$$

with $\mathcal{F}_{\pi^0\gamma^*\gamma^*}(q_1^2,q_2^2)=\mathcal{F}_{\pi^0\gamma^*\gamma^*}(q_2^2,q_1^2)$. Inserting the expression (5.23) into (5.21) and computing the corresponding Dirac traces in Eq. (5.22), we obtain

$$\begin{aligned}a_\mu^{(\mathrm{h.\;L\times L};\pi^0)} \;=\;& e^6\int\frac{d^4q_1}{(2\pi)^4}\int\frac{d^4q_2}{(2\pi)^4}\,\frac{1}{q_1^2q_2^2(q_1+q_2)^2[(p+q_1)^2-m^2][(p-q_2)^2-m^2]}\\ &\times\left[\frac{\mathcal{F}_{\pi^0\gamma^*\gamma^*}(q_1^2,(q_1+q_2)^2)\;\mathcal{F}_{\pi^0\gamma^*\gamma^*}(q_2^2,0)}{q_2^2-M_\pi^2}\;T_1(q_1,q_2;p)\right.\\ &\left.+\;\frac{\mathcal{F}_{\pi^0\gamma^*\gamma^*}(q_1^2,q_2^2)\;\mathcal{F}_{\pi^0\gamma^*\gamma^*}((q_1+q_2)^2,0)}{(q_1+q_2)^2-M_\pi^2}\;T_2(q_1,q_2;p)\right]\,,\end{aligned} \tag{5.25}$$

where $T_1(q_1,q_2;p)$ and $T_2(q_1,q_2;p)$ denote two polynomials in the invariants $p\cdot q_1$, $p\cdot q_2$, $q_1\cdot q_2$. Their expressions can be found in Ref. [104]. The former arises from the two first diagrams shown in Fig. 11, which give identical contributions, while the latter corresponds to the third diagram on this same figure. At this stage, it should also be pointed out that the expression (5.23) does not, strictly speaking, represent the contribution arising from the pion pole only. The latter would require that the numerators in (5.23) be evaluated at the values of the momenta that correspond to the pole indicated by the corresponding denominators. For instance, the numerator of the term proportional to $T_1(q_1,q_2;p)$ in Eq. (5.25) should rather read $\mathcal{F}_{\pi^0\gamma^*\gamma^*}(q_1^2,(q_1^2+2q_1\cdot q_2+M_\pi^2)\;\mathcal{F}_{\pi^0\gamma^*\gamma^*}(M_\pi^2,0)$ with $q_2^2=M_\pi^2$. However, Eq. (5.25) corresponds to what previous authors have called the pion pole contribution, and for the sake of comparison I shall adopt the same definition.

From here on, information on the form factor $\mathcal{F}_{\pi^0\gamma^*\gamma^*}(q_1^2,q_2^2)$ is required in order to proceed. The simplest model for the form factor follows from the Wess-Zumino-Witten (WZW) term [107, 108] that describes the Adler-Bell-Jackiw anomaly [109, 110] in chiral perturbation theory. Since in this case the form factor is constant, one needs an ultraviolet cutoff, at least in the contribution to Eq. (5.25) involving T_1, the one involving T_2 gives a finite result even for a constant form factor [100]. Therefore, this model cannot be used for a reliable estimate, but at best serves only

illustrative purposes in the present context.[17] Previous calculations [100, 101, 103] have also used the usual vector meson dominance form factor [see also Ref. [111]]. The expressions for the form factor $\mathcal{F}_{\pi^0\gamma^*\gamma^*}$ based on the ENJL model that have been used in Ref. [102] do not allow a straightforward analytical calculation of the loop integrals. However, compared with the results obtained in Refs. [100, 101, 103], the corresponding numerical estimates are rather close to the VMD case [within the error attributed to the model dependence]. Finally, representations of the form factor $\mathcal{F}_{\pi^0\gamma^*\gamma^*}$, based on the large-$N_C$ approximation to QCD and that takes into account constraints from chiral symmetry at low energies, and from the operator product expansion at short distances, have been discussed in Ref. [112] . They involve either one vector resonance [lowest meson dominance, LMD] or two vector resonances (LMD+V), see [112] for details. The four types of form factors just mentioned can be written in the form [F_π is the pion decay constant]

$$\mathcal{F}_{\pi^0\gamma^*\gamma^*}(q_1^2,q_2^2) \,=\, \frac{F_\pi}{3}\left[f(q_1^2) \,-\, \sum_{M_{V_i}} \frac{1}{q_2^2-M_{V_i}^2} g_{M_{V_i}}(q_1^2)\right]. \tag{5.26}$$

For the VMD and LMD form factors, the sum in Eq. (5.26) reduces to a single term, and the corresponding function is denoted $g_{M_V}(q^2)$. It depends on the mass M_V of the vector resonance, which will be identified with the mass of the ρ meson. For our present purposes, it is enough to consider only these two last cases, along with the constant WZW form factor. The corresponding functions $f(q^2)$ and $g_{M_V}(q^2)$ are displayed in Table 5.

Table 5: The functions $f(q^2)$ and $g_{M_V}(q^2)$ of Eq. (5.26) for the different form factors. N_C is the number of colors, taken equal to 3, and $F_\pi = 92.4$ MeV is the pion decay constant. Furthermore, $c_V = \frac{N_C}{4\pi^2}\frac{M_V^4}{F_\pi^2}$.

	$f(q^2)$	$g_{M_V}(q^2)$
WZW	$-\dfrac{N_C}{4\pi^2F_\pi^2}$	0
VMD	0	$\dfrac{N_C}{4\pi^2F_\pi^2}\dfrac{M_V^4}{q^2-M_V^2}$
LMD	$\dfrac{1}{q^2-M_V^2}$	$-\dfrac{q^2+M_V^2-c_V}{q^2-M_V^2}$

We may now come back to Eq. (5.25). With a representation of the form (5.26), the angular integrations can be performed, using for instance standard Gegenbauer polynomial techniques (hyperspherical approach), see Refs. [113, 114, 56]. This leads to a two-dimensional integral representation:

$$a_\mu^{(\mathrm{h.\ L\times L};\pi^0)} \,=\, \left(\frac{\alpha}{\pi}\right)^3\left[a_\mu^{(\pi^0;1)}+a_\mu^{(\pi^0;2)}\right], \tag{5.27}$$

$$a_\mu^{(\pi^0;1)} \,=\, \int_0^\infty dQ_1\int_0^\infty dQ_2\left[w_{f_1}(Q_1,Q_2)\; f^{(1)}(Q_1^2,Q_2^2) + w_{g_1}(M_V,Q_1,Q_2)\; g_{M_V}^{(1)}(Q_1^2,Q_2^2)\right], \tag{5.28}$$

[17] In the context of an effective field theory approach, the pion pole with WZW vertices represents a chirally suppressed, but large-N_C dominant contribution, whereas the charged pion loop is dominant in the chiral expansion, but suppressed in the large-N_C limit.

$$a_\mu^{(\pi^0;2)} = \int_0^\infty dQ_1 \int_0^\infty dQ_2 \left[\sum_{M=M_\pi, M_V} w_{g_2}(M, Q_1, Q_2)\, g_M^{(2)}(Q_1^2, Q_2^2) \right]. \quad (5.29)$$

The functions $f^{(1)}(Q_1^2, Q_2^2)$, $g_{M_V}^{(1)}(Q_1^2, Q_2^2)$, $g_{M_\pi}^{(2)}(Q_1^2, Q_2^2)$ and $g_{M_V}^{(2)}(Q_1^2, Q_2^2)$ are expressed in terms of the functions given in Table 5, see Ref. [104], where the universal [for the class of form factors that have a representation of the type shown in Eq. (5.26)] weight functions w in Eqs. (5.28) and (5.29) can also be found. The latter are plotted in Fig. 12.

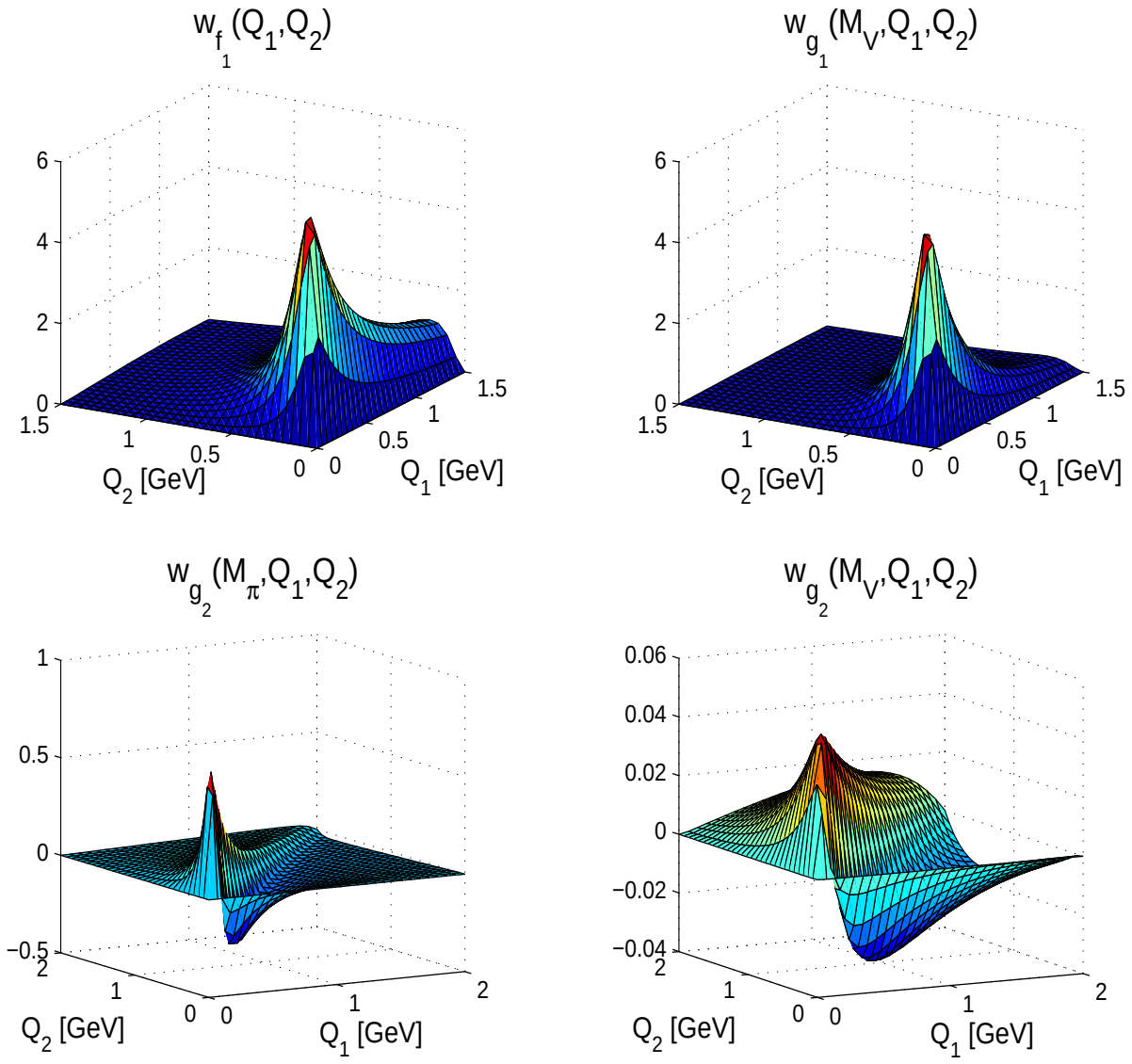

Figure 12: The weight functions appearing in Eqs. (5.28) and (5.29). Note the different ranges of Q_i in the subplots. The functions w_{f_1} and w_{g_1} are positive definite and peaked in the region $Q_1 \sim Q_2 \sim 0.5$ GeV. Note, however, the tail in w_{f_1} in the Q_1-direction for $Q_2 \sim 0.2$ GeV. The functions $w_{g_2}(M_\pi, Q_1, Q_2)$ and $w_{g_2}(M_V, Q_1, Q_2)$ take both signs, but their magnitudes remain small as compared to $w_{f_1}(Q_1, Q_2)$ and $w_{g_1}(M_V, Q_1, Q_2)$. We have used $M_V = M_\rho = 770$ MeV.

The functions w_{f_1} and w_{g_1} are positive and concentrated around momenta of the order of 0.5 GeV. This feature was already observed numerically in Ref. [102] by varying the upper bound of the integrals [an analogous analysis is contained in Ref. [101]]. Note, however, the tail in w_{f_1} in the

Q_1 direction for $Q_2 \sim 0.2$ GeV. On the other hand, the function w_{g_2} has positive and negative contributions in that region, which will lead to a strong cancellation in the corresponding integrals, provided they are multiplied by a positive function composed of the form factors [see the numerical results below]. As can be seen from the plots, and checked analytically, the weight functions vanish for small momenta. Therefore, the integrals are infrared finite. The behaviors of the weight functions for large values of Q_1 and/or Q_2 can also be worked out analytically. From these, one can deduce that in the case of the WZW form factor, the corresponding, divergent, integral for $a_\mu^{(\pi^0;1)}$ behaves, as a function of the ultraviolet cut off Λ, as $a_\mu^{(\pi^0;1)} \sim \mathcal{C} \ln^2 \Lambda$, with [104]

$$\mathcal{C} = 3 \left(\frac{N_C}{12\pi}\right)^2 \left(\frac{m_\mu}{F_\pi}\right)^2 = 0.0248\,. \tag{5.30}$$

The log-squared behavior follows from the general structure of the integral (5.28) for $a_\mu^{(\pi^0;1)}$ in the case of a constant form factor, as pointed out in [5]. The expression (5.30) of the coefficient $\mathcal{C}$ has been derived independently, in Ref. [115], through a renormalization group argument in the effective theory framework.

Table 6: Results for the terms $a_\mu^{(\pi^0;1)}$, $a_\mu^{(\pi^0;2)}$ and for the pion exchange contribution to the anomalous magnetic moment $a_\mu^{\mathrm{h.\ L\times L};\pi^0}$ according to Eq. (5.27) for the different form factors considered. In the WZW model we used a cutoff of 1 GeV in the first contribution, whereas the second term is ultraviolet finite.

Form factor	$a_\mu^{(\pi^0;1)}$	$a_\mu^{(\pi^0;2)}$	$a_\mu^{\mathrm{h.\ L\times L};\pi^0} \times 10^{10}$
WZW	0.095	0.0020	12.2
VMD	0.044	0.0013	5.6
LMD	0.057	0.0014	7.3

In the case of the other form factors, the integration over Q_1 and Q_2 is finite and can now be performed numerically. [18] Furthermore, since both the VMD and LMD model tend to the WZW constant form factor as $M_V \to \infty$, the results for $a_\mu^{(\pi^0;1)}$ in these models should scale as $\mathcal{C} \ln^2 M_V^2$ for a large resonance mass. This has been checked numerically, and the value of the coefficient $\mathcal{C}$ obtained that way was in perfect agreement with the value given in Eq. (5.30). The results of the integration over Q_1 and Q_2 are displayed in Table 6. They definitely show a sign difference when compared to those obtained in Refs. [100, 101, 103, 111], although in absolute value the numbers agree perfectly. After the results of Table 6 were made public [104], previous authors checked their calculations and soon discovered that they had made a sign mistake at some stage [105, 106]. Almost simultaneously, the results presented in Table 6 and in Refs. [104, 115] also received independent confirmations [117, 116].

The analysis of [104] leads to the following estimates

$$a_\mu^{\mathrm{h.\ L\times L};\pi^0} = 5.8(1.0) \times 10^{-10}\,, \tag{5.31}$$

and

$$a_e^{\mathrm{h.\ L\times L};\pi^0} = 5.1 \times 10^{-14}\,. \tag{5.32}$$

Taking into account the other contributions computed by previous authors, and adopting a conservative attitude towards the error to be ascribed to their model dependences, the total contribution to a_μ coming from the hadronic light-by-light scattering diagrams amounts to

$$a_\mu^{\mathrm{h.\ L\times L}} = 8(4) \times 10^{-10}\,. \tag{5.33}$$

[18] In the case of the VMD form factor, an analytical result is now also available [116].

5.3 Electroweak contributions to a_μ

Electroweak corrections to a_μ have been considered at the one and two loop levels. The one loop contributions, shown in Fig. 13, have been worked out some time ago, and read [118]-[122]

$$a_\mu^{\mathrm{W}(1)} = \frac{G_\mathrm{F}}{\sqrt{2}}\frac{m_\mu^2}{8\pi^2}\left[\frac{5}{3}+\frac{1}{3}\left(1-4\sin^2\theta_W\right)^2+\mathcal{O}\left(\frac{m_\mu^2}{M_Z^2}\log\frac{M_Z^2}{m_\mu^2}\right)+\mathcal{O}\left(\frac{m_\mu^2}{M_H^2}\log\frac{M_H^2}{m_\mu^2}\right)\right], \quad (5.34)$$

where the weak mixing angle is defined by $\sin^2\theta_W = 1 - M_W^2/M_Z^2$.

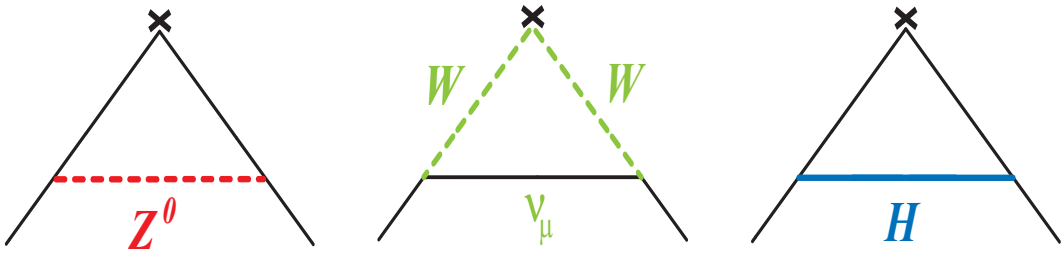

Figure 13: One loop weak interaction contributions to the anomalous magnetic moment.

Numerically, with $G_\mathrm{F} = 1.16639(1)\times 10^{-5}\,\mathrm{GeV}^{-2}$ and $\sin^2\theta_W = 0.224$,

$$a_\mu^{\mathrm{W}(1)} = 19.48\times 10^{-10}\,, \quad (5.35)$$

It is convenient to separate the two–loop electroweak contributions into two sets of Feynman graphs: those which contain closed fermion loops, which are denoted by $a_\mu^{\mathrm{EW}(2);\mathrm{f}}$, and the others, $a_\mu^{\mathrm{EW}(2);\mathrm{b}}$. In this notation, the electroweak contribution to the muon anomalous magnetic moment is

$$a_\mu^{\mathrm{EW}} = a_\mu^{\mathrm{W}(1)} + a_\mu^{\mathrm{EW}(2);\mathrm{f}} + a_\mu^{\mathrm{EW}(2);\mathrm{b}}\,. \quad (5.36)$$

I shall review the calculation of the two–loop contributions separately.

5.3.1 Two loop bosonic contributions

The leading logarithmic terms of the two–loop electroweak bosonic corrections have been extracted using asymptotic expansion techniques, see e.g. Ref. [123]. In the approximation where $\sin^2\theta_W \to 0$ and $M_H \sim M_W$ these calculations simplify considerably and one obtains

$$a_\mu^{\mathrm{EW}(2);\mathrm{b}} = \frac{G_\mathrm{F}}{\sqrt{2}}\frac{m_\mu^2}{8\pi^2}\frac{\alpha}{\pi}\times\left[-\frac{65}{9}\ln\frac{M_W^2}{m_\mu^2}+\mathcal{O}\left(\sin^2\theta_W\ln\frac{M_W^2}{m_\mu^2}\right)\right]. \quad (5.37)$$

In fact, these contributions have now been evaluated analytically, in a systematic expansion in powers of $\sin^2\theta_W$, up to $\mathcal{O}[(\sin^2\theta_W)^3]$, where $\ln\frac{M_W^2}{m_\mu^2}$ terms, $\ln\frac{M_H^2}{M_W^2}$ terms, $\frac{M_W^2}{M_H^2}\ln\frac{M_H^2}{M_W^2}$ terms, $\frac{M_W^2}{M_H^2}$ terms and constant terms are kept [75]. Using $\sin^2\theta_W = 0.224$ and $M_H = 250\,\mathrm{GeV}$, the authors of Ref. [75] find

$$a_\mu^{\mathrm{EW}(2);\mathrm{b}} = \frac{G_\mathrm{F}}{\sqrt{2}}\frac{m_\mu^2}{8\pi^2}\frac{\alpha}{\pi}\times\left[-5.96\ln\frac{M_W^2}{m_\mu^2}+0.19\right] = \frac{G_\mathrm{F}}{\sqrt{2}}\frac{m_\mu^2}{8\pi^2}\left(\frac{\alpha}{\pi}\right)\times(-79.3)\,, \quad (5.38)$$

showing, in retrospect, that the simple approximation in Eq. (5.37) is rather good.

5.3.2 Two loop fermionic contributions

The discussion of the two–loop electroweak fermionic corrections is more delicate. First, it contains a hadronic contribution. Next, because of the cancellation between lepton loops and quark loops in the electroweak $U(1)$ anomaly, one cannot separate hadronic effects from leptonic effects any longer. In fact, as discussed in Refs. [124, 125], it is this cancellation which eliminates some of the large logarithms which, incorrectly were kept in Ref. [126]. It is therefore appropriate to separate the two–loop electroweak fermionic corrections into two classes: One is the class arising from Feynman diagrams containing a lepton or a quark loop, with the external photon, a virtual photon and a virtual Z^0 attached to it, see Fig. 14.[19] The quark loop of course again represents non perturbative hadronic contributions which have to be evaluated using some model. This first class is denoted by $a_\mu^{\mathrm{EW}(2);\mathrm{f}}(\ell;q)$. It involves the QCD correlation function

$$W_{\mu\nu\rho}(q,k) = \int d^4x\, e^{iq\cdot x} \int d^4y\, e^{i(k-q)\cdot y} \langle\Omega\,|\mathrm{T}\{j_\mu(x)A_\nu^{(Z)}(y)j_\rho(0)\}|\Omega\rangle\,, \tag{5.39}$$

with k the incoming external photon four-momentum associated with the classical external magnetic field. As previously, j_ρ denotes the hadronic part of the electromagnetic current, and $A_\rho^{(Z)}$ is the axial component of the current which couples the quarks to the Z^0 gauge boson. The other class is defined by the rest of the diagrams, where quark loops and lepton loops can be treated separately, and is called $a_\mu^{\mathrm{EW}(2);\mathrm{f}}(\mathrm{residual})$.

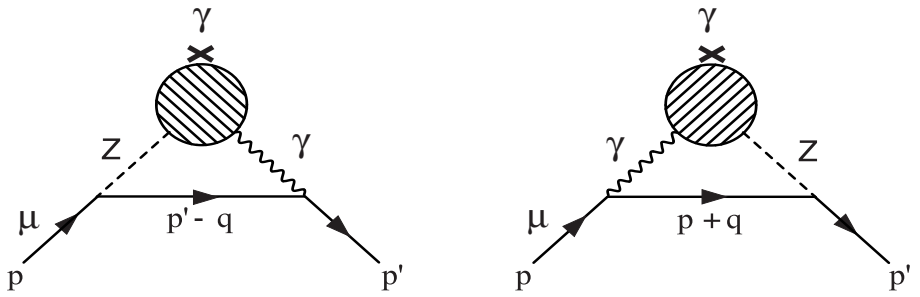

Figure 14: Graphs with hadronic contributions to $a_\mu^{\mathrm{EW}(2);\mathrm{f}}(\ell,q)$ and involving the QCD three point function $W_{\mu\nu\rho}(q,k)$.

The contribution from $a_\mu^{\mathrm{EW}(2);\mathrm{f}}(\mathrm{residual})$ brings in factors of the ratio m_l^2/M_W^2. It has been estimated, to a very good approximation, in Ref. [125], with the result

$$a_\mu^{\mathrm{EW}(2);\mathrm{f}}(\mathrm{residual}) \;=\; \frac{G_\mathrm{F}}{\sqrt{2}}\,\frac{m_\mu^2}{8\pi^2}\,\frac{\alpha}{\pi} \times \left[\frac{1}{2\sin^2\theta_W}\left(-\frac{5}{8}\frac{m_l^2}{M_W^2} - \log\frac{m_l^2}{M_W^2} - \frac{7}{3}\right) + \Delta_{\mathrm{Higgs}}\right]\,, \tag{5.40}$$

where Δ_{Higgs} denotes the contribution from diagrams with Higgs lines, which the authors of Ref. [125] estimate to be

$$\Delta_{\mathrm{Higgs}} = -5.5 \pm 3.7\,, \tag{5.41}$$

and therefore,

$$a_\mu^{\mathrm{EW}(2);\mathrm{f}}(\mathrm{residual}) \;=\; \frac{G_\mathrm{F}}{\sqrt{2}}\,\frac{m_\mu^2}{8\pi^2}\,\frac{\alpha}{\pi} \times [-21(4)]\,. \tag{5.42}$$

[19] If one works in a renormalizable gauge, the contributions where the Z^0 is replaced by the neutral unphysical Higgs should also be included. The final result does not depend on the gauge fixing parameter ξ_Z, if one works in the class of 't Hooft gauges.

Let us finally discuss the contributions to $a_\mu^{\mathrm{EW}(2);\mathrm{f}}(\ell;q)$. Here, it is convenient to treat the contributions from the three generations separately. The contribution from the third generation can be calculated in a straightforward way, with the result [124, 125]

$$\begin{aligned} a_\mu^{\mathrm{EW}(2);\mathrm{f}}(\tau;t,b) &= \frac{G_\mathrm{F}}{\sqrt{2}}\frac{m_\mu^2}{8\pi^2}\frac{\alpha}{\pi}\times\left[-3\ln\frac{M_Z^2}{m_\tau^2}-\ln\frac{M_Z^2}{m_b^2}-\frac{8}{3}\ln\frac{m_t^2}{M_Z^2}+\frac{8}{3}+\mathcal{O}\left(\frac{M_Z^2}{m_t^2}\ln\frac{m_t^2}{M_Z^2}\right)\right] \\ &= \frac{G_\mathrm{F}}{\sqrt{2}}\frac{m_\mu^2}{8\pi^2}\frac{\alpha}{\pi}\times(-30.6)\,. \end{aligned} \tag{5.43}$$

In fact the terms of $\mathcal{O}\left(\frac{M_Z^2}{m_t^2}\ln\frac{m_t^2}{M_Z^2}\right)$ and $\mathcal{O}\left(\frac{M_Z^2}{m_t^2}\right)$ have also been calculated in Ref. [125]. There are in principle QCD perturbative corrections to this estimate, which have not been calculated, but the result in Eq. (5.43) is good enough for the accuracy required at present. The contributions of the remaining charged standard model fermions involve the light quarks u and d, as well as the second generation s quark, for which non perturbative effects tied to the spontaneous breaking of chiral symmetry are important [124, 127]. The contributions from the first and second generation are thus most conveniently taken together, with the result

$$\begin{aligned} a_\mu^{\mathrm{EW}(2);\mathrm{f}}(e,\mu;u,d,s,c) &= \frac{G_\mathrm{F}}{\sqrt{2}}\frac{m_\mu^2}{8\pi^2}\frac{\alpha}{\pi}\times\left\{-3\ln\frac{M_Z^2}{m_\mu^2}-\frac{5}{2}\right. \\ &\qquad\qquad -3\ln\frac{M_Z^2}{m_\mu^2}+4\ln\frac{M_Z^2}{m_c^2}-\frac{11}{6}+\frac{8}{9}\pi^2-8 \\ &\quad\left.+\left[\frac{4}{3}\ln\frac{M_Z^2}{m_\mu^2}+\frac{2}{3}+\mathcal{O}\left(\frac{m_\mu^2}{M_Z^2}\ln\frac{M_Z^2}{m_\mu^2}\right)\right]-1.38(35)+0.06(2)\right\} \qquad (5.44) \\ &= \frac{G_\mathrm{F}}{\sqrt{2}}\frac{m_\mu^2}{8\pi^2}\frac{\alpha}{\pi}\times[-34.5(4)]\,, \qquad (5.45) \end{aligned}$$

where the first line shows the result from the e loop and the second line the result from the μ loop and the c quark, which is treated as a heavy quark. The term between brackets in the third line is the one induced by the anomalous term in the hadronic three point function $W_{\mu\nu\rho}(q,k)$ The other contributions have been estimated on the basis of an approximation to the large-N_C limit of QCD, similar to the one discussed for the two-point function $\Pi(Q^2)$ after Eq. (5.12), see Ref. [127] for details.

The result in Eq. (5.44) for the contribution from the first and second generations of quarks and leptons is conceptually very different to the corresponding one proposed in Ref. [125],

$$\begin{aligned} a_\mu^{\mathrm{EW}(2);\mathrm{f}}(\ell,q)(e,\mu;u,d,s,c) &= \frac{G_\mathrm{F}}{\sqrt{2}}\frac{m_\mu^2}{8\pi^2}\frac{\alpha}{\pi}\left[-3\ln\frac{M_Z^2}{m_\mu^2}+4\ln\frac{M_Z^2}{m_u^2}-\ln\frac{M_Z^2}{m_d^2}-\frac{5}{2}-6\right. \\ &\qquad \acute{o}\quad \left.-3\ln\frac{M_Z^2}{m_\mu^2}+4\ln\frac{M_Z^2}{m_c^2}-\ln\frac{M_Z^2}{m_s^2}-\frac{11}{6}+\frac{8}{9}\pi^2-6\right] \qquad (5.46) \\ &= \frac{G_\mathrm{F}}{\sqrt{2}}\frac{m_\mu^2}{8\pi^2}\frac{\alpha}{\pi}\times(-31.9)\,. \qquad (5.47) \end{aligned}$$

where the light quarks are, *arbitrarily*, treated the same way as heavy quarks, with $m_u = m_d = 0.3\,\mathrm{GeV}$, and $m_s = 0.5\,\mathrm{GeV}$. Although, numerically, the two results turn out not to be too different, the result in Eq. (5.46) follows from an hadronic model which is in contradiction with basic properties of QCD. This is at the origin of the spurious cancellation of the $\ln M_Z$ terms in Eq. (5.46).

Putting together the numerical results in Eqs. (5.38), (5.42), (5.43) with the new result in Eq. (5.44), we finally obtain the value

$$a_\mu^{\rm EW} = \frac{G_{\rm F}}{\sqrt{2}}\,\frac{m_\mu^2}{8\pi^2}\left[\frac{5}{3}+\frac{1}{3}\left(1-4\sin^2\theta_W\right)^2-\left(\frac{\alpha}{\pi}\right)(165.4(4.0)\right] = 15.0(1)\times 10^{-10}\,, \tag{5.48}$$

which shows that the two–loop correction represents indeed a reduction of the one–loop result by an amount of 23%. The final error here does not include higher order electroweak effects [128].

5.4 Comparison with experiment

We may now put all the pieces together and obtain the value for a_μ predicted by the standard model. We have seen that in the case of the hadronic vacuum polarization contributions, the latest evaluation [92] shows a discrepancy between the value obtained exclusively from e^+e^- data and the value that arises if τ data are also included. This gives us the two possibilities

$$\begin{aligned} a_\mu^{\rm SM}(e^+e^-) &= (11\,659\,169.1\pm 7.5\pm 4.0\pm 0.3)\times 10^{-10} \\ a_\mu^{\rm SM}(\tau) &= (11\,659\,186.3\pm 6.2\pm 4.0\pm 0.3)\times 10^{-10}\,, \end{aligned} \tag{5.49}$$

where the first error comes from hadronic vacuum polarization, the second from hadronic light-by-light scattering, and the last from the QED and weak corrections. When compared to the present experimental average

$$a_\mu^{\rm exp} = (11\,659\,203\pm 8)\times 10^{-10} \tag{5.50}$$

there results a difference,

$$\begin{aligned} a_\mu^{\rm exp} - a_\mu^{\rm SM}(e^+e^-) &= 33.9(11.2)\times 10^{-10}\,, \\ a_\mu^{\rm exp} - a_\mu^{\rm SM}(\tau) &= 16.7(10.7)\times 10^{-10}\,, \end{aligned}$$

which represents 3.0 and 1.6 standard deviations, respectively.

Although experiment and theory have now both reached the same level of accuracy, $\sim \pm 8\times 10^{-10}$ or 0.7 ppm, the present discrepancy between the e^+e^- and τ based evaluations makes the interpretation of the above results a delicate issue as far as evidence for new physics is concerned. Other evaluations of comparable accuracy [88, 90, 41] cover a similar range of variation in the difference between experiment and theory. One possibility to come to a conclusion would be to have the experimental result still more accurate, so that even the difference $a_\mu^{\rm exp} - a_\mu^{\rm SM}(\tau)$ would become sufficiently significant. In this respect, it is certainly very important that the Brookhaven experiment is given the means to improve on the value of $a_\mu^{\rm exp}$, bringing its error down to $\sim \pm 4\times 10^{-10}$ or 0.35 ppm. Furthermore, the value obtained for $a_\mu^{\rm SM}(e^+e^-)$ relies strongly on the low-energy data obtained by the CMD-2 experiment, with none of the older data able to check them at the same level of precision. In this respect, the prospects for additional high statistics data in the future, either from KLOE or from BaBar, are most welcome. On the other hand, if the present discrepancy in the evaluations of the hadronic vacuum polarization finds a solution in the future, and if the experimental error is further reduced, by, say, a factor of two, then the theoretical uncertainty on the hadronic light-by-light scattering will constitute the next serious limitation on the theoretical side. It is certainly worthwhile to devote further efforts to a better understanding of this contribution, for instance by finding ways to feed more constraints with a direct link to QCD into the descriptions of the four-point function $\Pi_{\mu\nu\rho\sigma}(q_1,q_2,q_3)$.

6 Concluding remarks

With this review, I hope to have convinced the reader that the subject of the anomalous magnetic moments of the electron and of the muon is an exciting and fascinating topic. It provides a good example of mutual stimulation and strong interplay between experiment and theory.

The anomalous magnetic moment of the electron constitutes a very stringent test of QED and of the practical working of the framework of perturbatively renormalized quantum field theory at higher orders. It tests the validity of QED at very short distances, and provides at present the best determination of the fine structure constant.

The anomalous magnetic moment of the muon represents the best compromise between sensitivity to new degrees of freedom describing physics beyond the standard model and experimental feasibility. Important progress has been achieved on the experimental side during the last couple of years, with the results of the E821 collaboration at BNL. The experimental value of a_μ is now known with an accuracy of 0.7ppm. Hopefully, the Brookhaven experiment will be given the opportunity to reach its initial goal of achieving a measurement at the 0.35 ppm level.

As can be inferred from the examples mentioned in this text, the subject constitutes, from a theoretical point of view, a difficult and error prone topic, due to the technical difficulties encountered in the higher loop calculations. The theoretical predictions have reached a precision comparable to the experimental one, but unfortunately there appears a discrepancy between the most recent evaluations of the hadronic vacuum polarization according to whether τ data are taken into account or not. Hadronic contributions, especially from vacuum polarization and from light-by-light scattering, are responsible for the bulk part of the final uncertainty in the theoretical value $a_\mu^{\rm SM}$. Further efforts are needed in order to bring these aspects under better control.

Acknowledgments

I wish to thank A. Nyffeler, S. Peris, M. Perrottet, and E. de Rafael for stimulating and very pleasant collaborations, and for sharing many insights on this vast subject and on related topics. Most of the figures appearing in this text were kindly provided by M. Perrottet, to whom I am also most grateful for a careful and critical reading of the manuscript. Finally, I wish to thank B. Duplantier and V. Rivasseau for the invitation to give a presentation at the "Séminaire Poincaré". This work is supported in part by the EC contract No. HPRN-CT-2002-00311 (EURIDICE).

References

[1] *Quantum Electrodynamics*, T. Kinoshita Ed., World Scientific Publishing Co. Pte. Ltd., 1990.

[2] J. Calmet, S. Narison, M. Perrottet and E. de Rafael, Rev. Mod. Phys. **49**, 21 (1977).

[3] A. Czarnecki and W. J. Marciano, Nucl. Phys. B (Proc. Suppl.) **76**, 245 (1998).

[4] V. W. Hughes and T. Kinoshita, Rev. Mod. Phys. **71**, S133 (1999).

[5] K. Melnikov, Int. J. Mod. Phys. A **16**, 4591 (2001).

[6] E. de Rafael, arXiv:hep-ph/0208251.

[7] A. Czarnecki and W. J. Marciano, Phys. Rev. D **64**, 013014 (2001).

[8] A list of recent papers on the subject can be found under the URL http://www.slac.stanford.edu/spires/find/hep/www?c=PRLTA,86,2227.

[9] L. L. Foldy, Phys. Rev. **87**, 688 (1952); Rev. Mod. Phys. **30**, 471 (1958).

[10] S. J. Brodsky and J. D. Sullivan, Phys. Rev. **156**, 1644 (1967).

[11] R. Barbieri, J. A. Mignaco and E. Remiddi, Nuovo Cimento **11A**, 824 (1972).

[12] T. Appelquist and J. Carazzone, Phys. Rev. D **11**, 2856 (1975).

[13] T. Sterling and M. J. Veltman, Nucl. Phys. **B 189**, 557 (1981).

[14] E. d'Hoker and E. Farhi, Nucl. Phys. **B 248**, 59, 77 (1984).

[15] T. Kinoshita, Nuovo Cimento **51B**, 140 (1967).

[16] B. E. Lautrup and E. de Rafael, Nucl. Phys. **B 70**, 317 (1974).

[17] E. de Rafael and J. L. Rosner, Ann. Phys. (N. Y.) **82**, 369 (1974).

[18] T. Kinoshita and W. J. Marciano, *Theory of the Muon Anomalous Magnetic Moment*, in [1], p. 419.

[19] J. E. Nafe, E. B. Nelson and I. I. Rabi, Phys. Rev. **71**, 914 (1947).

[20] H. G. Dehmelt, Phys. Rev. **109**, 381 (1958).

[21] R. S. Van Dyck, P. B. Schwinberg and H. G. Dehmelt, Phys. Rev. Lett. **59**, 26 (1987).

[22] R. S. Van Dyck, *Anomalous Magnetic Moment of Single Electrons and Positrons: Experiment*, in [1], p. 322.

[23] A. Rich and J. C. Wesley, Rev. Mod. Phys. **44**, 250 (1972).

[24] P. Kusch and H. M. Fowley, Phys. Rev. **72**, 1256 (1947).

[25] P. A. Franken and S. Liebes Jr., Phys. Rev. **104**, 1197 (1956).

[26] A. A. Schuppe, R. W. Pidd, and H. R. Crane, Phys. Rev. **121**, 1 (1961).

[27] D. T. Wilkinson and H. R. Crane, Phys. Rev. **130**, 852 (1963).

[28] G. Gräff, E. Klempt and G. Werth, Z. Phys. **222**, 201 (1969).

[29] J. C. Wesley and A. Rich, Phys. Rev. A **4**, 1341 (1971).

[30] R. S. Van Dyck, P. B. Schwinberg and H. G. Dehmelt, Phys. Rev. Lett. **38**, 310 (1977).

[31] F. J. M. Farley and E. Picasso, *The Muon g - 2 Experiments*, in [1], p. 479.

[32] J. Bailey et al., Phys. Lett. **B28**, 287 (1968).

[33] J. Bailey et al., Phys. Lett. **B55**, 420 (1975).

[34] J. Bailey et al. [CERN-Mainz-Daresbury Collaboration], Nucl. Phys. **B 150**, 1 (1979).

[35] R. M. Carey et al.,Phys. Rev. Lett. **82**, 1632 (1999).

[36] H. N. Brown et al. [Muon (g - 2) Collaboration], Phys. Rev. D **62**, 091101(R) (2000).

[37] H. N. Brown et al. [Muon (g - 2) Collaboration], Phys. Rev. Lett. **86**, 2227 (2001).

[38] G. W. Bennett et al. [Muon (g - 2) Collaboration], Phys. Rev. Lett. **89**, 101804 (2002); Erratum-ibid. **89**, 129903 (2002).

[39] K. Ackerstaff et al. [OPAL Collaboration], Phys. Lett. **B431**, 188 (1998).

[40] M. Acciarri et al. [L3 Collaboration], Phys. Lett. **B434**, 169 (1998).

[41] S. Narison, Phys. Lett. **B513**, 53 (2001); Erratum-ibid. **B526**, 414 (2002).

[42] J. Schwinger, Phys. Rev. **73**, 413 (1948); **76**, 790 (1949).

[43] R. Karplus and N. M. Kroll, Phys. Rev. **77**, 536 (1950).

[44] A. Peterman, Helv. Phys. Acta **30**, 407 (1957).

[45] C. M. Sommerfield, Phys. Rev. **107**, 328 (1957).

[46] C. M. Sommerfield, Ann. Phys. (N.Y.) **5**, 26 (1958).

[47] G. S. Adkins, Phys. Rev. D **39**, 3798 (1989).

[48] J. Schwinger, *Particles, Sources and Fields, VolumeIII*, Addison-Wesley Publishing Company, Inc., 1989.

[49] S. Laporta and E. Remiddi, Phys. Lett. **B379**, 283 (1996).

[50] R. Barbieri and E. Remiddi, Nucl. Phys. **B 90**, 233 (1975).

[51] M. A. Samuel and G. Li, Phys. Rev. D **44**, 3935 (1991).

[52] S. Laporta and E. Remiddi, Phys. Lett. **B265**, 181 (1991).

[53] S. Laporta, Phys. Rev. D **47**, 4793 (1993).

[54] S. Laporta, Phys. Lett. **B343**, 421 (1995).

[55] S. Laporta and E. Remiddi, Phys. Lett. **B356**, 390 (1995).

[56] R. Z. Roskies, E. Remiddi and M. J. Levine, *Analytic evaluation of sixth-order contributions to the electron's g factor*, in [1], p. 162.

[57] T. Kinoshita, *Theory of the anomalous magnetic moment of the electron – Numerical Approach*, in [1], p. 218.

[58] J. Aldins, S. J. Brodsky, A. Dufner, and T. Kinoshita, Phys. Rev. Lett. **23**, 441 (1970); Phys. Rev. D **1**, 2378 (1970).

[59] S. J. Brodsky and T. Kinoshita, Phys. Rev. D **3**, 356 (1971).

[60] J. Calmet and M. Perrottet, Phys. Rev. D **3**, 3101 (1971).

[61] J. Calmet and A. Peterman, Phys. Lett. **B47**, 369 (1973).

[62] M. J. Levine and J. Wright, Phys. Rev. Lett. **26**, 1351 (1971); Phys. Rev. D **8**, 3171 (1973).

[63] R. Carroll and Y. P. Yao, Phys. Lett. **B48**, 125 (1974).

[64] P. Cvitanovic and T. Kinoshita, Phys. Rev. D **10**, 3978, 3991, 4007 (1974).

[65] T. Kinoshita and W. B. Lindquist, Phys. Rev. D **27**, 867, 877, 886 (1983); D **39**, 2407 (1989); D **42**, 636 (1990).

[66] M. Caffo, S. Turrini, and E. Remiddi, Phys. Rev. D **30**, 483 (1984).

[67] E. Remiddi and S. P. Sorella, Lett. Nuovo Cim. **44**, 231 (1985).

[68] T. Kinoshita, IEEE Trans. Instrum. Meas. **44**, 498 (1995).

[69] H. Suura and E. Wichmann, Phys. Rev. **105**, 1930 (1957).

[70] A. Peterman, Phys. Rev. **105**, 1931 (1957).

[71] H. H. Elend, Phys. Lett. **20**, 682 (1966); Erratum-ibid. **21**, 720 (1966).

[72] B. E. Lautrup and E. de Rafael, Phys. Rev. **174**, 1835 (1968).

[73] S. Laporta, Nuovo Cimento **106A**, 675 (1993).

[74] S. Laporta and E. Remiddi, Phys. Lett. **B301**, 440 (1993).

[75] A. Czarnecki, B. Krause and W. J. Marciano, Phys. Rev. Lett. **76**, 3267 (1996).

[76] P. J. Mohr and B. N. Taylor, Rev. Mod. Phys. **72**, 351 (2000).

[77] B. Krause, Phys. Lett. **B390**, 392 (1997).

[78] C. Bouchiat and L. Michel, J. Phys. Radium **22**, 121 (1961).

[79] L. Durand III, Phys. Rev. **128**, 441 (1962); Erratum-ibid. **129**, 2835 (1963).

[80] J. Z. Bai et al. [BES Collaboration], Phys. Rev. Lett. **84**, 594 (2000); Phys. Rev. Lett. **88**, 101802 (2000).

[81] R. R. Akhmetshin et al. [CMD-2 Collaboration], Phys. Lett. **B527**, 161 (2002).

[82] R. Barate et al. [ALEPH Collaboration], Z. Phys. **C 2**, 123 (1997).

[83] S. Anderson et al. [CLEO Collaboration], Phys. Rev. D **61**, 112002 (2000).

[84] S. Eidelman and F. Jegerlehner, Z. Phys. C **67**, 585 (1995).

[85] D. H. Brown and W. A. Worstell, Phys. Rev. D **54**, 3237 (1996).

[86] R. Alemany, M. Davier and A. Höcker, Eur. Phys. J. **C 2**, 123 (1998).

[87] M. Davier and A. Höcker, Phys. Lett. **B419**, 419 (1998).

[88] M. Davier and A. Höcker, Phys. Lett. **B435**, 427 (1998).

[89] G. Cvetic, T. Lee and I. Schmidt, Phys. Lett. **B513**, 361 (2001).

[90] J. F. de Trocóniz and F. J. Ynduráin, Phys. Rev. D **65**, 093001 (2002).

[91] F. Jegerlehner, arXiv:hep-ph/0104304.

[92] M. Davier, S. Eidelman, A. Höcker and Z. Zhang, arXiv:hep-ph/0208177.

[93] M. Perrottet and E. de Rafael, unpublished.

[94] K. Hagiwara, A. D. Martin, D. Nomura and T. Teubner, arXiv:hep-ph/0209187.

[95] S. Peris, M. Perrottet and E. de Rafael, JHEP **05**, 011 (1998).

[96] G. 't Hooft, Nucl. Phys. **B 72**, 461 (1974).

[97] E. Witten, Nucl. Phys. **B 160**, 157 (1979).

[98] M. Perrottet and E. de Rafael, private communication.

[99] J. Calmet, S. Narison, M. Perrottet and E. de Rafael, Phys. Lett. **B61**, 283 (1976).

[100] T. Kinoshita, B. Nizic, Y. Okamoto, Phys. Rev. D **31**, 2108 (1985).

[101] M. Hayakawa, T. Kinoshita and A. I. Sanda, Phys. Rev. Lett. **75**, 790 (1995); Phys. Rev. D **54**, 3137 (1996).

[102] J. Bijnens, E. Pallante and J. Prades, Nucl. Phys. **B 474**, 379 (1996).

[103] M. Hayakawa and T. Kinoshita, Phys. Rev. D **57**, 465 (1998).

[104] M. Knecht and A. Nyffeler, Phys. Rev. D **65**, 073034 (2002).

[105] M. Hayakawa and T. Kinoshita, arXiv:hep-ph/0112102, and the erratum to [103] published in Phys. Rev. D **66**, 019902(E) (2002).

[106] J. Bijnens, E. Pallante and J. Prades, Nucl. Phys. **B 626**, 410 (2002).

[107] J. Wess and B. Zumino, Phys. Lett. **B37**, 95 (1971).

[108] E. Witten, Nucl. Phys. **B 223**, 422 (1983).

[109] S. L. Adler, Phys. Rev. **177**, 2426 (1969).

[110] J. S. Bell and R. Jackiw, Nuovo Cimento A **60**, 47 (1969).

[111] J. Bijnens and F. Persson, arXiv:hep-ph/0106130.

[112] M. Knecht and A. Nyffeler, Eur. Phys. J. C **21**, 659 (2001).

[113] J. L. Rosner, Ann. Phys. (N.Y.) **44**, 11 (1967). Implicitly, the method of Gegenbauer polynomials was already used in the following papers: M. Baker, K. Johnson, and R. Willey, Phys. Rev. **136**, B1111 (1964); **163**, 1699 (1967).

[114] M. J. Levine and R. Roskies, Phys. Rev. D **9**, 421 (1974); M. J. Levine, E. Remiddi, and R. Roskies, *ibid.* **20**, 2068 (1979).

[115] M. Knecht, A. Nyffeler, M. Perrottet and E. de Rafael, Phys. Rev. Lett. **88**, 071802 (2002).

[116] I. Blokland, A. Czarnecki and K. Melnikov, Phys. Rev. Lett. **88**, 071803 (2002).

[117] W. J. Bardeen and A. de Gouvea, private communication.

[118] W.A. Bardeen, R. Gastmans and B.E. Lautrup, Nucl. Phys. **B 46**, 315 (1972).

[119] G. Altarelli, N. Cabbibo and L. Maiani, Phys. Lett. **B40**, 415 (1972).

[120] R. Jackiw and S. Weinberg, Phys. Rev. D **5**, 2473 (1972).

[121] I. Bars and M. Yoshimura, Phys. Rev. D **6**, 374 (1972).

[122] M. Fujikawa, B.W. Lee and A.I. Sanda, Phys. Rev. D **6**, 2923 (1972).

[123] V.A. Smirnov, Mod. Phys. Lett. A **10**, 1485 (1995).

[124] S. Peris, M. Perrottet and E. de Rafael, Phys. Lett. **B355**, 523 (1995).

[125] A. Czarnecki, B. Krause and W. Marciano, Phys. Rev. D **52**, R2619 (1995).

[126] T.V. Kukhto, E.A. Kuraev, A. Schiller and Z.K. Silagadze, Nucl. Phys. **B 371**, 567.

[127] S. Peris, M. Perrottet and E. de Rafael, arXiv:hep-ph/0205102.

[128] G. Degrasi and G.F. Giudice, Phys. Rev. D **58** (1998) 053007.